SYNTHESIS, CHARACTERIZATION, AND CHELATION PROPERTIES TOWARD HEAVY METAL IONS OF A CHITOSAN–LINKED 1-HYDROXY-2- PYRIDINETHIONE POLYMER

By
Faryza Jamil Muhanna

Supervisor
Dr. Kamal I. Abu-Dari, Prof.

Co-Supervisor
Dr. Mohammad S. Mubarak, Prof.

This Thesis was Submitted in Partial Fulfillment of the Requirements for the Degree of Master of Science in Chemistry.

Faculty of Graduate Studies
University of Jordan

May, 2011

COMMITTEE DECISION

This Thesis/Dissertation (Synthesis, Characterization, and Chelation Properties Toward Heavy Metal Ions of a Chitosan–linked 1-hydroxy-2- pyri dinethione Polymer) was Successfully Defended and Approved on 27/04/2011.

The Examination Committee	**Signature**
Dr. Kamal I. Abu-Dari, (Supervisor) Prof. Inorganic Chemistry	------------------
Dr. Mohammad S. Mubarak, (Co-Supervisor) Prof. of Organic Chemistry	------------------
Dr. Manar K. Fayyad, (Member) Prof. of Analytical Chemistry	------------------
Dr. Haythem A. Saadeh, (member) Assoc. professor of Organic Chemistry	------------------
Dr. Khalil J. Asali, (External Member) Prof. of Inorganic Chemistry (Jordan University of Science and Technology)	------------------

DEDICATION

To

My Family
Parents , Brothers , Sisters

And

To my dearest friends

Sabreen Wahab
&
Isra' Aqeel

ACNOWLEDGMENT

During my study in the University of Jordan, so many people have been supporting, helping, and encouraging me on the road toward obtaining my Master degree.

I must extend my deep gratitude to my best supervisors Prof. Kamal Abu-Dari and Prof. Mohammad Mubarak for their considerable assistance, advice and guidance.

Thanks due to the members of the examination committee; Prof. Dr. Manar K. Fayyad, Dr. Haythem Saadeh & Prof. Dr. Khalil Al-Asali for their suggestions & comments.

I am deeply grateful to my colleagues with whom I spent the course of graduate studies, for their excellent suggestions and contributions to the completion of this work, Manal Al-Khabbas, Smah Ata, and Dana Alshaer.

I would, also, like to thank staff members, and employees at the chemistry department/university of Jordan for their assistance to complete this work.

LIST Of CONTENTS

LIST OF TABLES

LIST OF FIGURES

LIST OF ABBREVIATIONS

AAS: Atomic Absorption Spectroscopy

α: The chemisorption rate at zero coverage (mg g^{-1} min^{-1})

β: Freundlich isotherm constant and equal 1/n which is a measure of heterogeneity of the surface and usually less than unity and n refers to the adsorption intensity

C_e: Equilibrium concentration of adsorbate in solution (mg/L)

C_o: Initial metal concentration.

DTG: Differential Thermogravimetric.

DSC: Differential Scanning Calorimetery.

Eq. Conc.: Equilibrium concentration.

FTIR: Fourier Transform Infrared.

ΔG°: Change in standard Gibbs free energy.

ΔH°: Change in standard enthalpy.

k_1: Equilibrium rate constant of the pseudo first order adsorption (min^{-1})

k_2: Equilibrium rate constant of the pseudo-second-order kinetic model (g/mg h).

K_d: Distribution coefficient.

K_L: Langmuir constant.

K_F: Freundlich isotherm constant ($(L/mg)^{1/n}$) .

Kp: The intraparticle diffusion rate constant (mg/(g $h^{1/2}$))

n: Freundlich constant relates to adsorption intensity .

N: The number of data points

Particle size: Will be denoted as large-particle size resin (250 μ -500 μ), and particle size (60 μ -125 μ) will be denoted as small-particle size resin.

ppm: Parts per million.

q: Metal ion adsorbed in

mg per gram of adsorbent.

q_m: Monolayer adsorption capacity.

R^2: Correlation coefficient.

R: The ideal gas constant.

SEM : Scanning Electron Microscope.

Resin: Chitosan-linked 1-hydroxy-2-pyridinethione-4-carboxylic acid

V: Volume of the solution

ΔS°: Change in standard entropy of adsorption.

SSE, %: Sum of squared errors and gives the validity of each kinetic model.

TGA: Thermogravimetric Analysis

x_i: Interaparticle diffusion constant proportional to the boundary layer   thickness (mg/g)

SYNTHESIS, CHARACTERIZATION, AND CHELATION PROPERTIES TOWARD HEAVY METAL IONS OF A CHITOSAN–LINKED 1-HYDROXY-2- PYRIDINETHIONE POLYMER

By
Faryza Jamil Muhanna

Supervisor
Dr. Kamal I. Abu-Dari, Prof.

Co-Supervisor
Dr. Mohammad S. Mubarak, Prof.

ABSTRACT

The chelation behavior of the chitosan-linked 1-hydroxy-2-pyridinethione-4-carboxylic acid towards heavy metal ions in aqueous solutions was studied by a batch equilibration technique as a function of contact time, pH, polymer mass and metal concentration. The amount of metal ion uptake of the resin was determined by using atomic absorption spectroscopy (AAS), and the highest uptake was achieved at pH 7.0. The isothermal behavior and the kinetics of adsorption of metal(II) ions on this polymer with respect to the initial mass of the polymer and temperature were also investigated; Langmuir and Freundlich adsorption models were applied to describe the experimental isotherms and isotherm constants.

1. Introduction

1.1 An Overview

Contamination of water by heavy metals is a serious environmental problem, mainly due to the discharge of industrial waste (Yurdakoc, 2005). Heavy metals are highly toxic even at low concentrations and can accumulate in living organisms, causing several disorders and diseases (Gotoh, 2004). Among all the heavy metal ions, special attention has been given to lead(II). Lead(II) ions can be found in effluents from battery recycling plants, lead mining and electronic assembly plants. Lead is known to affect the function of central nervous system, interferes with the protein of many enzymes, including those responsible for causing sever anemia. Once lead enters into the body fluid it accumulates in liver, kidney, spleen, bone marrow, and bones. Copper(II) ions although known to be an essential trace element to humans, have fatal effect if induced at high dosage (Wan and Fatinathan, 2009).

Though a set of regulations have been approved that prohibit unsupervised disposal of metal ions, we still notice that metal ions emerge in a variety of wastewaters stemming from catalysts, electrical apparatus, painting and coating, extractive metallurgy, antibacterials, insecticides and fungicides, photography, pyrotechnics, smelting, metal electroplating, fertilizer, mining, pigments, stabilizers, alloy industries, electrical wiring, plumbing, heating, roofing and construction piping, water purification, gasoline additives, cable covering, ammunition and battery industries and sewage sludge.

To reduce metal content of industrial waste, experts recommend using many techniques such as chemical precipitation, ion exchange, membrane filtration, electrolytic methods, reverse osmosis, solvent extraction, and adsorption (Kocaoba, 2005; Zhoua, 2009). However, these methods are limited by high operational cost and/or may also be

inefficient in the removal of some toxic metal ions, mainly at trace level concentrations (Yurdakoc, 2005; Monier, et al. 2010).

The use of chelating resins is one of the best methods of metal removal. Chelating resins are easily regenerated and differ from activated carbon and ion exchange resins in their high selectivity in sorption processes (Donia, 2008). Attention has recently been focused on chitosan and its derivatives as bioadsorbents. Chitosan is a major component of crustacean shells and one of the most abundant biopolymers in nature (Sarhan, 2009). It is known for its ability to uptake several metal ions with mechanisms that depend on the type of metal ion and the pH of the solution (Monier, et al., 2010).

1.2 Metal -Ligand Affinity

Binding of a metal ion to a polymer depends on many factors such as the functionality of the chelating group, the density of chelating groups, oxidation state and electronic configuration of the metal, stereochemistry of steric constraints as well as electrostatic interactions (Zalloum, 2008). As previously discussed, the chelating functionality usually consists of some type of mono-, bi-, or polydentate moiety with nitrogen and/or charged or neutral oxygen and sulfur groups that can act as Lewis bases and donate electrons to the metal ion.

The spacing between the functional groups attached to the polymer can play an important role on how the ligands chelate to metal ions. If the donor groups are close together on the polymer chain, or if there is little steric hindrance between chains, several donor atoms can act as bridging ligands. Thus, the metal ion can induce local folding or crosslinking of the polymer chains. In addition, the nature of the intervening groups is also important (Micioi, 2007). Small, flexible spacing groups aid in the

folding of the polymer chains, while rigid or bulky groups prohibit such activity. The bulkiness of the functional group itself also determines the steric constraints on metal ligation.

The pKa of the polymeric backbone and ligating groups attached to the polymer also has a significant effect on the metal-ligand interaction (Li, 2008). Many of the polymers bearing nitrogen functionalities experience very weak binding to metal cations at low pH due to protonation of the amine group; causing loss of nitrogen ability to bind to metal ions (Rivas, 2007). Increasing the pH above pKa for carboxylic acid functional groups causes deprotonation and increases electron donating ability. Furthermore, charge repulsion between similarly charged groups on the polymer can cause electrostatic repulsion which can affect the ligation efficacy as well.

The size, electronic configuration, and oxidation state of the metal ion affect the coordination geometry and coordination number. Metals with large ligand field stabilization energies such as d^3 and low spin d^6 prefer octahedral arrangements because the octahedral higher stabilization energy than tetrahedral and square planar. whereas metals such as Zn^{2+} with d^{10} configurations tend to have tetrahedral geometry (Atkins, 2006). The Pearson scale, a measure of the hardness or softness of species in terms of electron donation, suggests which types of chelate groups and metal ions will preferentially interact. Based on this scale, metal ions such as Hg(II), Pb(II), and Cd(II) ion are defined as soft acceptors and preferentially interact with soft donors such as sulfur. On the other hand, Cr(III) and Fe(III) ions are defined as a hard species and are best ligated by hard oxygen and nitrogen species (Lebrun, 2007). The interplay of the aforementioned parameters, which affect metal ligation affinity, can be employed for selective binding of metal ions.

1.3 Selectivity

Because most wastewater and soils contain a complex mixture of metallic ions, the selectivity or ability of the polymeric ligand to discriminate binding of metal ions is critical for successful remediation. Separation of target ions allows for proper waste disposal or recycling of these materials. In addition, many of these waste streams contain competing ligands such as ethylenediaminetetraacetic acid ($EDTA^{2-}$) which can compete with the chelating polymer to bind target metals and may be acidic and thus protonate the ligand and inactivate the donating ability of the polymer (Li, 2008).

One might tailor various parameters to selectively remove the target ion even in the presence of competitor ligands. For competing ligands, the pH of the solution can be altered to reduce the affinity of the metal for the competitor ligand. For competing metal ions, ligand substitution kinetics can be taken into account in the design of the chelating group and experimental conditions such as reaction time and temperature for the target metal ion removal. In addition, depending on the relative size of the target ion, encapsulating ligand functional groups can be utilized to create a size specific cage to trap the target metal ion (Bell, 2006; Micioi, 2007).

1.4 Types of Ligands

Most of the chelating polymers are selective for groups of metal ions rather than for a specific metal ion (Vernon and Nyo, 1978; Sugiii et al., 1979). The selectivity of a given resin is attributed to the differences in the stability constants of the different complexes formed with the ligand on the resin. This selectivity can be modified either by changing the analytical conditions of the metal solution, e.g. pH, temperature

(Buckley, 1985; Ebraheem, 2000; and Ebraheem, 2001), or by the addition of different complexing agents (Schmuckler, 1976).

Chelating resins act as multidentate chelating agents, creating one or more four, five- or six-membered rings (Gregor et al., 1952). A suitable chelating group for incorporation into a polymeric matrix must have the following general properties:

1. Capability of resin formation by incorporating into the repeating units of the polymer backbone by polymerization of a suitable monomer containing the required chelating group, or substitution into a polymeric matrix such chelating may be covalently bound to a polymer matrix.

2. Sufficient chemical stability so that it is not destroyed or altered during the polymerization reaction.

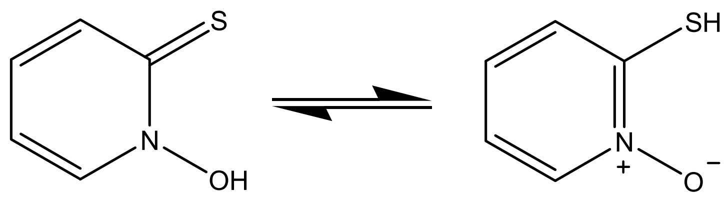
3. Sterically, the reagent should be compacted so that the formation of chelate rings would not be hindered by the matrix. The degree of crosslinking and other properties of the resin must be controlled to prevent steric hindrance to the formation of chelate rings (Vernon, 1977). In order for complexation or sorption to occur, it is not sufficient for functional groups to be present on the surface; they must also be accessible for chelation with the metal ion without steric hindrance. Thus, within chelating resin particles, many surface functional groups may remain inactive (Kantipuly et al., 1990).

The nature of the metal species and the functional group and/or donor atom capable of forming complexes with metal ions are of fundamental importance in extraction systems. The functional group atoms capable of forming chelate rings usually include oxygen, nitrogen, and sulfur. Nitrogen can be present in primary, secondary or tertiary amines, azo, diazo, nitrile, amide and other groups. Oxygen is usually in the form of phenolic,

carbonyl, carboxylic, hydroxyl, ether, and some other groups. Sulfur is in the form of thiol, thioester, thiocarbamate, and disulphide groups.

1.4.1 1-Hydroxy-2-pyridinethione.

1-hydroxy-2-pyridinethione was the first cyclic thiohydroxamic acid synthesized. On the basis of spectroscopic measurements, this ligand is thought to exist mainly as 1-hydroxy-2-pyridinethione tautomer (1a), rather than 2-mercapto-pyridine-1-oxide tautomer (1b) (Bond and Jones, 1999).



(1a) **(1b)**

Figure 1. 1-Hydroxy-2-pyridinethione tautomeric forms

The ligand 1-hydroxy-2-pyridinethione as well as its derivatives have been found to act as excellent complexing agents because these ligands contain both hard oxygen and soft sulfur donor atoms (Abu-Dari, et al., 1988; Abu-Dari and Raymond, 1990; Abu-Dari, et al., 1993). Various metal complexes of 1-hydroxy-2-pyridinethione, and derivatives of 1-hydroxy-2-pyridinethione-4-carboxylic and 1-hydroxy-2-pyridinethione-6-carboxylic have been prepared and characterized; these includes rhodium (III), palladium(II), lead(II) and cadmium(II), iron (III) and thorium(1V) and uranium(VI). (Abu-Dari, 1988; Abu-Dari, et al., 1991; Abu-Dari, et al., 1993; Abu-Dari and Raymond, 1990; Xiong, et al., 1996, and Casellato, U., et al., 1983).

1.4.2 1-Hydroxy-2-pyridinethione-4-carboxylic acid

1-Hydroxy-2-pyridinethione-6-carboxylic and 1-hydroxy-2-pyridinethione-4-carboxylic acid have been used to prepare new sequestering agents for iron and other metal ions that contain mono, di, tri and tetra hydroxyl pyridinthione ligating groups. These sequestering agents were prepared by binding 1-hydroxy-2-pyridinethione-6-carboxylic acid or 1-hydroxy-2-pyridinethione-4-carboxylic to the amines or amino acids through the formation of an amide bond through its carboxyl group (Abu-Dari and Rymond, 1990; Al-Thawabieh, 2004; Al-Khabbas, 2007).

1.5 Classification of chelating polymers according to their origin

1.5.1 Synthetic chelating polymers

Synthesis of chelating ion-exchange resins has begun in 1952 when Gregor synthesized the first member of a new class of ion-exchange resins in which chelating groups where introduced in highly cross-linked form (Vernon, 1977). Many synthetic chelating polymers have been prepared by the incorporation of chelating agents into a variety of polymeric matrices. This class is based on the nature of the chemical reaction employed in the polymerization process (Nicholson, 1997).

Synthetic chelating polymers can be classified according to their polymerization mechanism into two major types: Addition and condensation polymers (Carothers, 1929; Nicholson, 2006).

1.5.1.1 Addition polymerization

Addition polymers are those formed by the addition reaction of an unsaturated monomer, such as those reactions that take place in the polymerization of vinyl chloride:

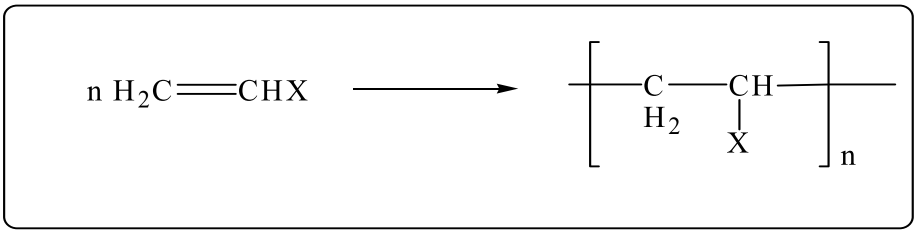


Figure 2. Addition polymerization of vinyl monomer

1.5.1.2 Condensation polymerization

Condensation polymers are those prepared from monomers where the reaction is accompanied by the loss of a small molecule, usually water, for example polyesters which are formed by condensation of alcohols and carboxylic acids as shown in the following reaction.

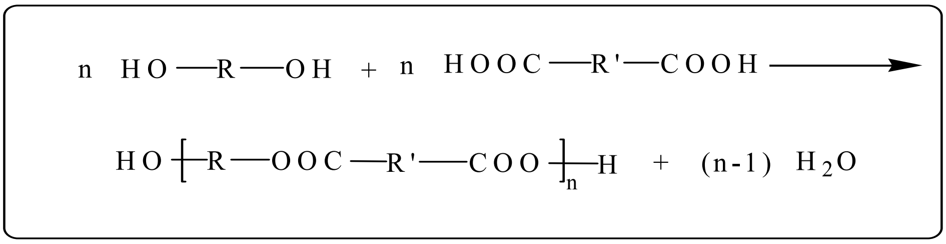


Figure 3. Synthesis of polyesters by condensation polymerization

1.5.2 Naturally Occurring Polymers

Naturally occurring chelating polymers include cellulose and its derivatives, starch, alginic acid, chitin, proteins, nucleic acids, humic acid, and lignin. Biopolymers are potential adsorbents and have received attention for being inexpensive, biodegradable, non-toxic, efficient (Wana et.al., 2010). Addition of function groups can be achieved either by modification after polymerisation, or by copolymerisation of suitable monomers with a conventional monomer (Cunliffe, 2004).

Chitin, (poly[b-(1-4)-2-acetoamido-2-deoxy-D-glucopyranose]), is the second most abundant polysaccharide after cellulose. It is readily available from seafood, crustacean shells and from fungi cell walls. Because of its insolubility in the vast majority of common solvents, chitin was considered an attractable polymer and for many years remained mainly as laboratory curiosity. However, as will be shown below, presently chitin and its derivative chitosan have become polymers of great interest in a large variety of areas of human activity.

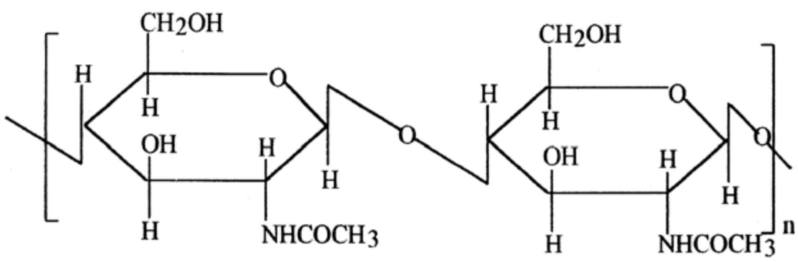


Figure 4. Chitin

Chitosan, composed mainly of poly(β-1-4)-2-amino-2-deoxy-D-glucopyranose is obtained from fully or partially deacetylated chitin. The pK_b of chitosan in aqueous

solutions in the range of 6.5-6.7 (Qu, 2000) and it has three types of reactive functional groups: an amino group at the C-2 position and primary and secondary hydroxyl groups at the C-3 and C-6 positions, respectively. At relatively low pH (< 6.5), chitosan is highly positively charged because of the protonation of the amino groups.

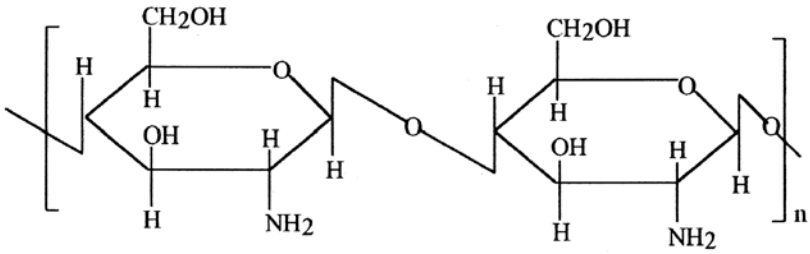


Figure 5. Chitosan

Chitosan is insoluble in water, but it dissolves in aqueous solutions of organic acids as acetic, formic, citric acid, and aqueous solutions of inorganic acids, as diluted hydrochloric acid, resulting in viscous solutions (Rinaudo et al., 1999).

On the other hand, at pH values = 6.5 and higher, the amino groups become deprotonated, which means that chitosan loses its positive charge and tends to precipitate from solution.

Other factor effect the solubility of chitosan is the degree of acetylation and molecular weight (Jiang, 2003; Jose´, 2005).

Chitosan can interact with anionic surfactants to form either soluble or insoluble complexes depending on solution conditions. It has been proposed that these complexes are stabilized by a combination of electrostatic, ion-dipole, and hydrophobic interaction (Masubon et al., 2004).

1.6 Application of chelating polymers

The driving force for much of the excitement surrounding chitin and chitosan is due to their potential applications and uses. Table 1 lists some examples of the known and potential applications of chitin, chitosan and their derivatives that have caught the imagination of scientists, raw material producers and manufacturers and users alike (Collier and Camp, 2000).

Table 1. Applications of chitin, chitosan and their derivatives

Application area	**Specific use**
Water treatment	Coagulating/flocculating agents for polluted waste waters
	Removal/recovery of metal ions from aqueous waste water
Agriculture	Plant elicitor
	Antimicrobial agents
	Plant seed coating
	Fertilizer
Textile and paper	Fibers for textile and woven fabrics
	Paper and film
Biotechnology	Chromatography packing
	Enzyme immobilizing materials
Food/Health Supplements	Natural thickeners
	Food additives including pet food
	Food processing (e.g. in sugar refining)
	Filtration and clarification
	Hypocholesterolemic agent (slimming agents)
Cosmetic	Ingredients for hair and skin care (conditioners)
Biomedical	Burns and wounds dressings for humans and animals
	Biomaterial (e.g. absorbable sutures)
	Anticoagulant or antithrombogenic materials(as sulfated-chitin derivatives)
	Hemostatic agents (as chitosan)
	Drug delivery, gene delivery

Source: Eugene, 2001

1.7 Adsorption isotherm Theory

Equilibrium isotherms are both fundamentally and commercially important to correlate equilibrium data between the various metal ions and chitosan in order to assess chitosan's capacity for chelation or desorption of different metal ions and as prerequisite for the design of commercial treatment systems. The more complex is the wastewater composition, more accuracy is needed in describing and selecting of the isotherm systems. Most research studies, based on chitosan adsorption, report the testing and results of single component ion systems.

Equilibrium isotherm equations are used to describe experimental sorption data. The equation parameters and the underlying thermodynamic assumptions of these equilibrium models often provide some insight into both the sorption mechanism and the surface properties and affinity of the sorbent. A substantial review of available literature isotherms is presented. The importance of obtaining the "best-fit" isotherm becomes more and more significant. As more applications are developed, more accurate and detailed isotherm description are required for the design of chitosan treatment systems.

For example, in the case of a multicomponent metal ion system the multicomponent equilibrium isotherms are needed for design purpose, and these are usually derived from the ideal adsorbed solution theory, which requires a very accurate description of the single-component equilibrium data. Therefore more attention should be given to the analysis of single component isotherm. The main isotherms are now reviewed with some discussion on the use of error analyses with isotherm data. (Gerente, et al., 2007)

1.7.1 Langmuir equation

The most widely used isotherm equation for modeling equilibrium data is the Langmuir (1918); for dilute solutions the Langmuir formula is represented by the following equation:

$$q = \frac{q_m K_L . \mathrm{C_e}}{(1 + K_L . C_e)} \tag{1}$$

Where C_e represents the equilibrium concentration of adsorbate in solution (ppm) and q and q_m are the equilibrium concentration of adsorbate adsorbed per unit mass of adsorbent (mg/g) and the Langmuir monolayer capacity, respectively. The parameter K_L is the langmuir isotherm constant (L/g).

When the concentration Ce $\rightarrow$ 0, then $1+K_L.Ce \rightarrow 1$. Then, Eq. (1) becomes a linear isotherm (G. McKay and J. F. proter, 1997).

The parameters of this model can be obtained by suitable linearization procedures followed by regression analysis as given in the following equations:

Linearized langmuir form (I):

$$K_L = q / \mathrm{Ce} = q_m K - Kq \tag{2}$$

Thus a plot of q/c_e against q should give a straight line with a slope = -K and an intercept = $q_m K$ if Langmuir equation is applicable (Sposito, 1984).

Other linear forms of Langmuir result from taking the inverse of equation (1);

Linearized Langmuir form (2)

$$1/q = \left(\frac{1}{(q_m K_L)}\right)\frac{1}{\mathrm{C_e}} + \frac{1}{q_m} \tag{3}$$

or by multiplying equation (3) by C_e;

Linearized Langmuir form (III)

$$\frac{C_e}{q} = \frac{1}{(q_m K_L)} + \left(\frac{1}{q_m}\right) C_e \quad (4)$$

(Mckay and Porter, 1997)

The Langmuir equation is applicable to homogenous sorption where each metal ion-check sorption process has equal sorption activation energy. The Langmuir equation obeys Henry's law concentrations (McKay and Proter, 1997).

1.7.2 Freundlich adsorption

The most important multi-site adsorption isotherm for heterogeneous surfaces is the Freundlich (1906) adsorption isotherm equation:

$$q = K_F Ce^{\beta} = K_F Ce^{1/n} \quad (5)$$

Where K_F ((L/mg)$^{1/n}$) is Freundlich isotherm constant and n is the Freundlich isotherm exponent constant. K_F is correlated to the maximum adsorption capacity and n gives an indication of how favorable the adsorption process is (Chiou and Ya-Li, 2002; Stevenson, 1982). The form 1/n emphasizes that C_e is raised to power less than unity. When this equation is expressed in the logarithmic form, a linear relationship is obtained. When the data are plotted as log q vs log C_e, the intercept is equal to log K_F and the slope is 1/n which is represented in the equation below.

log q = log K_F + 1/n log C_e (Schitizer, 1978).

The K_F parameter is related to the adsorption capacity, while β = 1/n which is a measure of heterogeneity of the surface and usually less than unity and n refers to the adsorption intensity. The Freundlich constant n also indicates the degree of favorability

of adsorption (Fuqiang et al., 2004). The constant K_F also provides an indication of the extent of adsorption and has some times been used in correlation studies for determining the relative importance of the various soil properties on adsorption (Stevenson, 1982).

Theoretically, the Freundlich equation represents a situation in which the quantity of solute adsorbed increases indefinitely with increasing concentration. This will occur when multilayers are formed. Also, heterogeneous sorption sites are implied (Stevenson, 1982; Yah-Shan, 2003).

1.7.3 Kinetic models

Four kinetic models, pseudo-first-order, pseudo-second-order, Elovich equation and intraparticle diffusion model are used to fit the experimental data. The mathematical description of theses models is given below. The conformity between data predicted by any of these models and the experimental data is indicated by the correlation coefficient R^2. The model of higher values of R^2 means that it more successfully describes the adsorption kinetics.

The differential form of the pseudo-first-order kinetic model could be expressed by the following equation (Igwe, 2007):

$$\frac{dQ_t}{Qe - Qt} = k_1 dt \qquad (6)$$

where t is the time (min) and k_1 is the equilibrium rate constant of the pseudo first order adsorption (min^{-1}). Integrating equation (6) by applying the boundary conditions, $t = 0$ to $t = t$ and $Q_t = 0$ to $Q_t = Q_e$, yields the following integral equation:

$$\log Q_e / (Q_e - Q_t) = 0.4342 k_1 t \qquad (7)$$

The value of the model parameters k_1 can be determined by plotting log (Q_e - Q_t) versus t to give a straight line of slope -0.4342 k_1 and intercept of log Q_e.

The differential form of the pseudo-second-order kinetic model is expressed by the following equation (Ho, 1998):

$$\frac{dQ_t}{dt} = k_1 (Q_e - Q_t)^2 \tag{8}$$

where k_2 is the equilibrium rate constant of the pseudo-second-order kinetic model (g/mg h). Integration of equation (8) between the boundary conditions of equation (6) yields the following equation:

$$t / Q_t = 1 / k_2 (Q_e)^2 + t / Q_e \tag{9}$$

The value of k_2 can be determined by plotting t/Q_t versus t to obtain a straight line of slope $1/Q_e$ and intercept of $1/(k_2\, Q_e^2)$.

The Elovich model was initially used to describe the adsorption of gases on solids (Low, 1960), however, the application of this model in liquid phase adsorption is gaining popularity. The differential form of this model is given below:

$$\frac{dQ_t}{dt} = \alpha \exp(-\beta Q_t) \tag{10}$$

where α is the chemisorption rate at zero coverage (mg g^{-1} min^{-1}) and β is the desorption rate constant (mg g^{-1} min^{-1}) during each experiment. Integrating equation (11) between the same boundary conditions will give the following equation:

$$Q_t = (\frac{1}{\beta}) \ln(\alpha\beta) + \frac{1}{\beta} \ln t \tag{11}$$

The values of α and β can be determined by plotting Q_t versus ln t which gives a straight line of slope $1/\beta$ and an intercept of $1/\beta \ln (\alpha\beta)$.

Since the above three models cannot give definite mechanisms for the adsorption process, another simplified model that represents the intra-particle diffusion model is tested (Wu, 2001). This model, which is based on the theory proposed by Weber and Morris assumes that the intraparticle mass transfer resistance is the rate determining

step which means that the adsorption process is pore diffusion controlled (Webwe, 1962). According to this theory the initial rates of interaparticle diffusion can be obtained from the following equation:

$$Q_t = x_i + k_p t^{1/2} \qquad (12)$$

where x_i is a constant proportional to the boundary layer thickness, (mg/g), k_p is the intraparticle diffusion rate constant (mg/(g $h^{1/2}$)) (Kavitha, 2007). For pore diffusion controlled sorption, a plot of Q_t versus $t^{1/2}$ gives a straight line of slope k_p and an intercept of x_i.

The adsorption kinetics of Pb^{+2} onto the chitosan was verified at different initial concentration. The validity of each model was determined by the sum of squared errors (SSE, %) given by:

$$SSE = \sqrt{\frac{\sum \left(Q_{e,\exp.} - Q_{e,cal.}\right)^2}{N}} \qquad (13)$$

where N is the number of data points. The lower the value of SSE the better a fit is.

1.7.4 Thermodynamics of adsorption on resin

In order to understand the possible adsorption mechanism involved in the removal process, thermodynamic functions for the system, including changes in Gibbs free energy (ΔG^o), change in enthalpy of adsorption (ΔH^o) and changes in entropy of adsorption (ΔS^o), were calculated using the following equation

$$\ln K_d = \Delta S^o/R - \Delta H^o/RT \qquad (14)$$

Where K_d is the equilibrium constant or distribution coefficient is defined as the amount of metal ion in the sorbed form on the resin phase divided by its amount in solution (Tompkin et al., 1947).

Mathematically;

$$K_d = \frac{\text{Conc. of metal ion sorbed or retained (mg /L)} \times V}{\text{Conc. of metal ion in solution (mg /L)} \times m} \quad (L/g)$$

$$K_d = \frac{(Co - Ceq) \times V}{Ceq \times m} \quad \text{(Covelo et al., 2007).}$$

where m $_{resin}$ and m $_{solution}$ are the fractions in mg of the metal ion on the resin and liquid in the phase, respectively. R is the gas constant and T is the temperature in Kelvin. The plot of $\ln K_d$ against 1/T for each metal ion gives a linear relationship, where the values of enthalpy (ΔH^o) were entropy (ΔS^o) are obtained from the slope and intercept of $\ln K_d$ vs. 1/T plots.

ΔG^o was calculated at each temperature using the following equation:

$$\Delta G^o = \Delta H^o - T\,\Delta S^o \qquad (15)$$

Aim of present work

To study the chelation properties of the chitosan-linked 1-hydroxy-2-pyridinethione-4-carboxylic acid resin towards the divalent transition metal ions (Pb^{2+}, Cu^{2+}, Zn^{2+}, Ni^{+2}, and Cd^{2+}) in aqueous solutions by batch equilibration technique as a function of contact time, pH, mass of resin, and concentration of metal ions. The amount of metal-ion uptake of the polymer will be determined using atomic absorption spectrometry (AAS).

2. Experimental

2.1 Materials and Chemicals

Unless otherwise indicated all chemicals were obtained from commercial sources and were used as received. *p*-Anisaldehyde (97.5%), trifluoroacetic acid (99%), and chitosan, medium molecular weight (2-amino-2-deoxy-β-D-glucan or glucosamine), were obtained from Aldrich. 2-Chloroisonicotinic acid was obtained from Fluorochem. Acetic acid and sodium acetate anhydrous (98.0%) were purchased from GCC (U.K.) Copper(II) acetate dihydrate, Cu.$(CH_3COO)_2$. $2H_2O$, (98%) and cadmium(II) chloride dihydrate,$CdCl_2.2H_2O$,(97%) were supplied by Fluka, (Switzerland). Nickel(II) acetate tetrahydrate, $Ni(CH_3COO)_2.4H_2O$, (98%), was obtained from BDH and zinc(II) acetate dihydrate metal salt, $Zn(CH_3COO)_2.2H_2O$, from Merck (Germany) and lead acetate trihydrate, $Pb(CH_3COO)_2.3H_2O$ (>99%) was purchased from Riedel – De Haën AG (Germany). Sodium perchlorate (99.0%) was obtained from Riedel-de Haen, acetic anhydride (97.5%), was obtained from Scharlau, pyridine (99.5%) were obtained from LAB-SCAN, Ireland, 1,1-carbonyldiimidazole (97%) was obtained from Acros (USA). Methanol, acetonitrile, acetic acid, hydrochloric acid (37%), sulphuric acid (98.07) were obtained from Merck (Germany). Hydrogen peroxide (30%), were obtained from Analyte Reagent, UK, nitric acid and dimethylformamide (DMF) were obtained from Tedia (USA).

Water was prepared in the Analytical Laboratory of Pharmaquestjo (Amman- Jordan) by reversed osmosis, followed by deionization to a conductivity 3.75 µS , and filtration with a Sartorius 0.2 µm filtration apparatus.

2.2 Instrumentation

Infrared spectra were recorded with a Nicolet Impact 400 FTIR-Spectrophotometer (4000- 400 cm^{-1}) using KBr pellets. Atomic absorption data were obtained using a Varian Atomic Absorption Spectrophotometer (AAS). Samples were shaken and thermostated using GFL-1083 shaker. Thermogravimetric analyses (TGA) were acquired with the aid of a NETZSCH STA 209 PC thermal analyzer. A Inolab pH meter model 720 A was employed for pH measurements. Elemental analyses were obtained with a Euro EA3000 CHNS-O elemental analyzer (Milian, Italy).

2.3 Synthesis of ligand

1-Hydroxy-2-pyridinethione-4-carboxylic acid was prepared, purified, and characterized according to unpublished procedure (Al-khabbas 2007; Ata, 2009).

2.4 Preparation of modified chitosan

N-[*p*-methoxy-benzyliden] poly-D-glucoseamine (I)

This compound was prepared according to published procedures (Zalloum, 2009) which involves addition of 6.4 g of *p*-anisaldehyde to a stirred solution of 10.00 g of chitosan in 100 mL of sodium hydroxide (1 M). At the end of the addition a white solid appears, which after cooling in ice bath, was collected, washed with ice cold water and cold ethanol-ether and dried to yield the title compound in high yield and degradation of polymer at 270 ^{o}C (decomposition). The IR spectrum of the prepared polymer is in agreement with its proposed structure. The intense broad bands in the 3200-3500 cm^{-1} region in the spectra are attributed to the intramolecular hydrogen bonded O-H stretching vibration and to the N-H group. The strong absorption bands in the 1620-1640 cm^{-1}

region are attributed to the (C=N) vibrations characteristic of imines which are not observed in chitosan. In addition, there was no evidence of bands characteristic of the free aromatic aldehydes near 1665 cm^{-1}. The absorption bands at in the 1540–1590 cm^{-1} region, which are not present in the original chitosan sample, are to the C=C stretching in the aromatic ring of the aldehyde. Moreover, bands at 1155 and 895 cm^{-1} are assigned to the polysaccharide structure of chitosan.

Diacetyl-N-[p-methoxy-benzyliden]-poly-D-glucoseamine (II)

To a stirred and cold solution of 5.00 g of N-[*p*-Methoxy-benzyliden]-poly-D-glucoseamine (I), in 50 mL of dry pyridine was added drop-wise 35 mL of acetic anhydride over 1 hour and then over night at room temperature. The reaction mixture was then poured onto an ice-water (400 mL) slowly with stirring. The product was collected as white powder, washed repeatedly with cold water and dried to yield the title compound in high yield. The IR spectrum shows disappearance of the peak of hydroxyl group in the 3200-3500 cm^{-1} of the prepared polymer and the appearance of band at 1750 due to C=O stretching.

Diacetyl poly-D-glucoseamine (III)

An amount of 3.30 g of diacetyl –N-[*p*-methoxy-benzyliden]-poly-D-glucoseamine (II) was dissolved in acetone (13 mL) and warmed up just to boiling. And then HCl (5 M, 3.1 mL) was added resulting in immediate formation of a precipitate. After cooling ether was added (50 mL) and the solution kept at 0 ^oC for 1 hour. The product was collected, washed with cold ether to yield the product in 85 % yield, and degradation of polymer at 200-205 ^oC (decomposition) (Henryk, M. et al., 2003). IR shows

disappearance of the bands in the 1620-1640 cm^{-1} region attributed to the (C=N) and the intense broad bands in the 3200-3500 cm^{-1} region in the spectra are attributed to the N-H group

2.5 Immobiliazation of 1-hydroxy-2-pyridinethione-4-carboxylic on acetylated chitosan, preparation of resin

A solution of 1,1-carbonyldiimidazole (4.74 g, 29.2 mmol) in DMF (50 mL) was added to a solution of 1-hydroxy-2-pyridinethione-4-carboxylic acid (5.0 g, 29.2 mmol) in DMF (20 mL) under N_2; the color changed from green to red with evolution of CO_2 gas. The solution was stirred under N_2 for 15 min, and diacetyl-poly-D-glucoseamine (4.28 g, 29.2 mmol) in DMF (20 mL) was added. The color changed to yellowish green and the solution was stirred overnight under N_2. Most of the DMF was then evaporated under reduced pressure and water (300 mL) was added. The product was collected by filtration, washed with ethanol and acetone, respectively. After soxhlet extraction with methanol for 24 hours, the resulting solid resin (green) was dried at 70 ^{o}C for 24 hours and sieved through mesh size (250-500 µm) and (125-60 µm). Satisfactory elemental analyses were obtained: Anal. calc for $[C_{16}H_{18}N_2O_8S]_n$: %C 48.24, %H 4.55, %N 7.03, %S 8.05 ; found : %C 47.81, %H 5.01, %N 7.20, %S 7.02.

2.6 Preparation of buffer solutions

A series of acetate buffer solutions was prepared from sodium acetate and acetic acid to obtain pH values ranging from 3.0 to 7.0. The ionic strength was maintained at a constant value of 0.10 M by the addition of the required amount of sodium perchlorate. The desired pH value was achieved by changing sodium acetate to acetic acid ratio, at a fixed ionic strength, according to the following equation.

$$pH = pKa + \log\frac{[acetate]}{[acetic\ acid]}$$

the pH of the resulting buffer solutions was checked with a pH meter (with an error less than ±0.05). Table 2 presents the amount of sodium acetate, acetic acid and sodium perchlorate used, such that the total ionic strength in Pb(II), Cu(II), Cd(II), Ni(II) or Zn(II) ions uptake runs remain at 0.10 M . (Equal volumes of 25.0 mL, of both the buffer and the standard metal ion solutions were used).

Table 2. Concentration of buffer components

pH	[Acetate] M	[Acetic acid] M	[$NaClO_4$] M	Ionic strength
3.0	0.1	5.62	0.1	0.4
3.5	0.1	1.77	0.1	0.4
4.0	0.1	0.56	0.1	0.4
5.0	0.1	0.06	0.1	0.4
6.0	0.1	5.60×10^{-3}	0.1	0.4
7.0	0.1	5.60×10^{-4}	0.1	0.4

2.7 Sample blank

Sample blank prepared by addition 25 ml of buffer with 25 mg lead (II) ions and measured directly and after 24 hrs.

Result showed no appreciable change in lead concentration.

2.8 Isothermal Behavior

Adsorption isotherms

The adsorption of Pb(II), Cu(II), Cd(II), Ni(II) and Zn(II) were carried out by weighing 0.1000 gram of dry resin, measured to the nearest 0.0003 g, which was later equilibrated with 25.0 mL of sodium acetate-acetic acid buffer of pH = 7.0 for 2 hours of continuous shaking. Then 25 mL samples of Pb(II), Cu(II), Cd(II), Ni(II) and Zn(II) solutions of different concentrations ranging from 40 ppm-1000 ppm were added to produce a total of 50 mL solutions containing 1.0-25.0 mg of metal ion and were shaken again for 12 hours at different temperatures of 15.0 °C, 25.0 °C, and 35.0 °C.

2.9 Chelation Characteristics of the Resins

2.9.1 Extent of metal-ion uptake

The Pb(II), Cu(II), Cd(II), Ni(II) and Zn(II) chelation characteristics were studied by the batch equilibrium technique. These experiments were carried out using 0.1000 gram of dry resin samples which were equilibrated with 25.0 mL solution of sodium acetate buffer of pH = 7.0 for 2 hours of continuous shaking. An amount of 25.0 ml containing 25.0 mg of metal ion was then added and the mixtures were shaken at 25°C for a specific period of time (0.083-24 hrs). The samples were filtered out and the amount of metal ion remaining in solution was determined by atomic absorption spectrophotometry (AAS) using standard solutions for calibration.

2.9.2 Effect of pH on the metal-ion uptake

Similar experiments were carried out in different buffer solutions with pH ranging from 3.0 to 7.0, at constant exposure time of 6 hours to determine the effect of pH on the metal ion uptake of resin.

2.9.3 Effect of metal mass on the metal-ion uptake

The effect of metal mass was studied by shaking 0.1000 g of resin with 25.0 mL of the acetate buffer solution at pH = 7.0 for 2 hours. A 25.0 mL of different masses of 2.50, 5.00, 10.00, 15.00, 20.00, and 25.00 mg of metals solution was then added and the mixtures were shaken at 25°C for an extra 6 hours. The samples were filtered out and the amount of metal ion remaining was determined by atomic absorption spectrophotometry (AAS).

2.9.4 Effect of polymer mass on the metal-ion uptake

The effect of polymer mass was studied by shaking different masses of 0.1000, 0.2000, 0.4000, 0.6000, 0.8000 gram of the dry resins with 25.0 mL of the acetate buffer solution at pH = 7.0 for 2 hours. A 25.0 mL solution containing 25.0 mg of metal ion was then added and the mixtures were shaken at 25 °C for an extra 6 hours. The samples were filtered out and the amount of metal ion remaining was determined by atomic absorption spectrophotometry (AAS).

2.10 Column Experiment

We employed a glass column of 150 mm length and 10 mm internal diameter for the present investigation. An amount of 0.50±0.0001) g of dry resin in 50 mL of acetate-buffer of pH 7 was used to pack the column in and the resin was then allowed to swell for 24 h. The acetate buffer was allowed to flow out of the column at a flow rate of 0.1 mL/min. A sample volume of 50 mL containing 1000 ppm of Pb(II) was passed through the column at the same flow rate and the concentration of the metal ion in the eluent

was determined by atomic absorption spectrophotometry. The same procedure was applied for the determination of Cu(II) and Zn(II) ions.

2.11 Desorption Studies

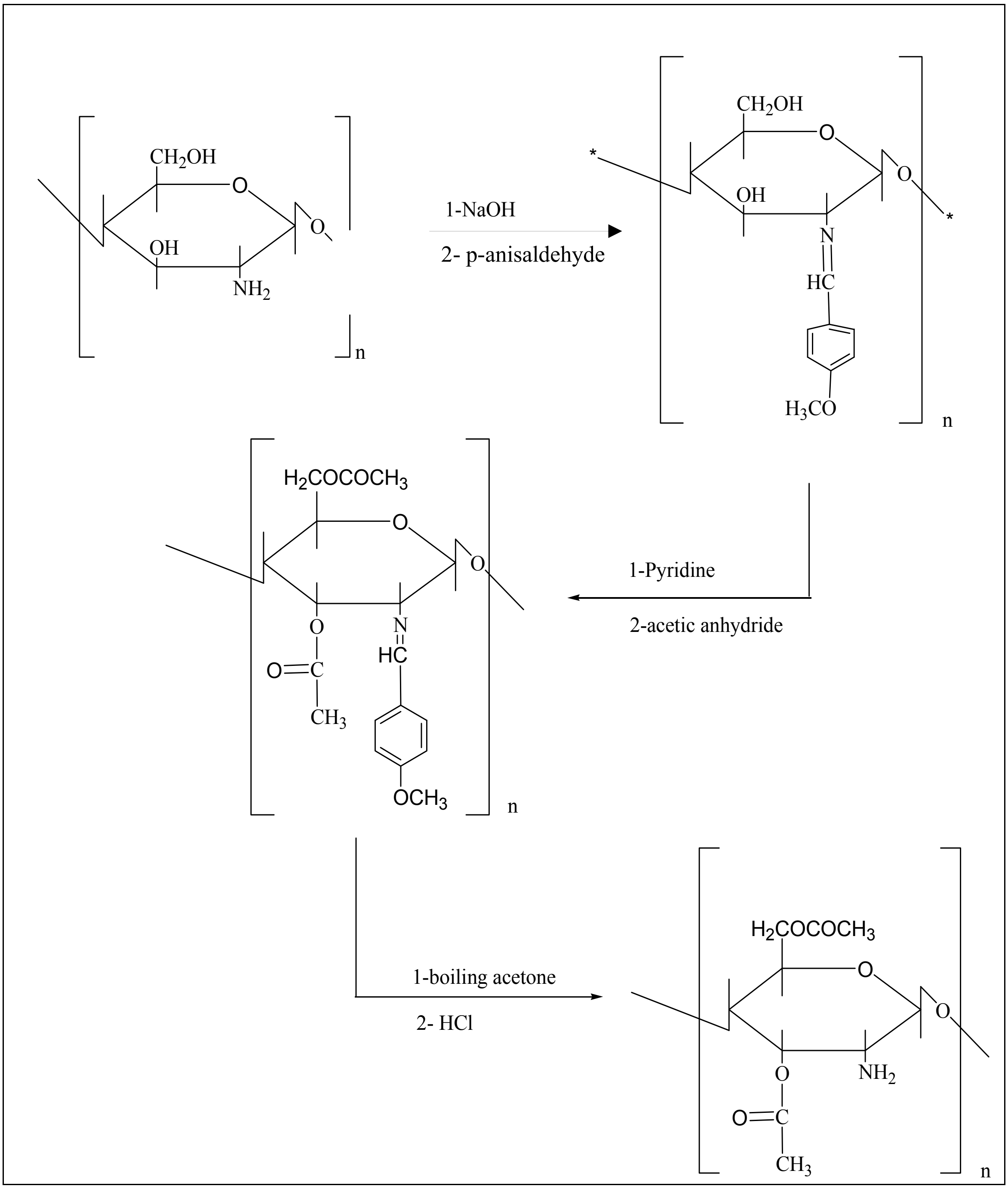
Desorption of metal ions from the resin loaded with each metal ion was studied under column conditions by paassing 50 mL of each of the following eluting agents through the column at a flow rate of 1mL/min : 1 M HNO_3, 0.5 M H_2SO_4, and 0.1 M EDTA 50 mL. The metal ion in the eluate was collected in and the concentration was determined with atomic absorption spectrophotometry.

3. Results and Discussion

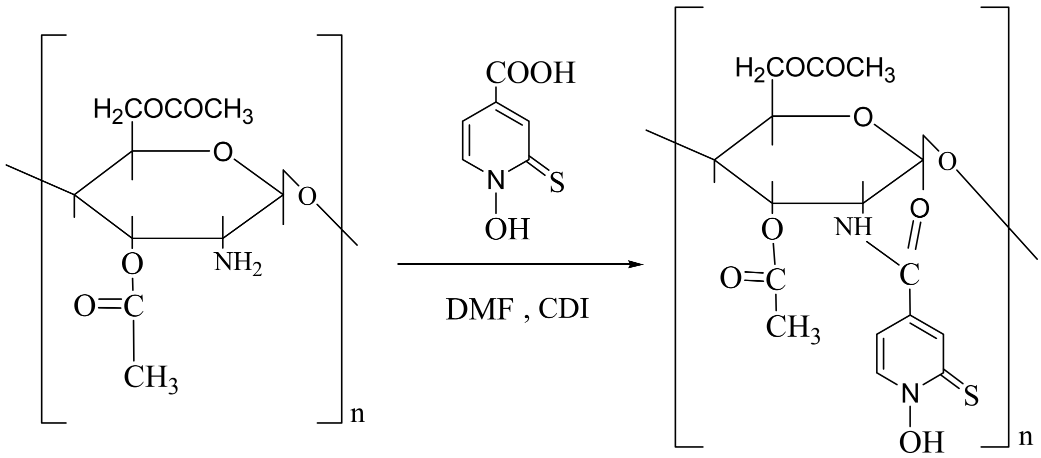
3.1 Synthesis and characterization of polymers

3.1.1 Synthesis

Chitosan is modified by linking its amine groups with 1-hydroxy-2-pyridinethione-4-carboxylic acid according to schemes 1 and 2 to produce a polymer capable of complexing specific metallic ions species with potential analytical and environmental applications (Hall and Yalpani, 1980; Rodrigues et al., 1998).



Scheme 1. Synthesis of acetylated chitosan



Scheme 2. Immobilization of 1-hydroxy-2-pyridinethione-4-carboxylic on acetylated chitosan.

3.1.2 Characterization of the modified chitosan resin

Characterization of resin and its metal chelates is of prime importance, since it provides good information about the structure of these resins. Several techniques can be employed to characterize the resins such as solubility, FTIR spectroscopy, elemental analysis and TGA.

3.1.2.1 Solubility

The resin is insoluble in water and in common organic solvents like DMF, DMSO, acetone, chloroform, dichloromethane, benzene, pyridine and acetonitrile. The resin is only slightly soluble in concentrated HCl which makes it difficult to use certain spectroscopic techniques, such as NMR, for characterization.

3.1.2.2 Water content or water regain (α)

Water regain, α, is defined as the amount of water adsorbed by 1.00 g of resin. The water regain parameter (α) provides an indirect measurement of the hydrophilic character of resins (Zulloum, 2009). A high α may indicate the presence of microporous hydrophilic sites, which provide the water-transport channels required for the effective sorption of metal ions from aqueous solutions. Samples of dry resin were suspended in water, and were left for a period of 2 hours and 24 hours. Then, the polymer was filtered, weighed, and dried at 80 ^{o}C in a vacuum oven and re-weighed. Water regain (α) can be calculated using the following equation:

$$\alpha = \frac{\text{mass of polymer bound water (g)}}{\text{mass of dry polymer (g)}}$$

The results of water regain ratio for the resin gg^{-1} are presented in Table 3.

Table 3. Water regain (α) in gg^{-1}units for large and small particle resin

Time (hr)	α of Small-particle resin	α of Large-particle resin
After 2 hrs.	1.73	1.35
After 24 hrs.	2.54	1.63

3.1.2.3. FTIR spectroscopy

The FTIR spectra of 1-hydroxy-2-pyridinethione-4-carboxylic acid, chitosan, acetylated chitosan and chitosan-linked 1-hydroxy-2-pyridinethione-4-carboxylic acid resin are displayed in Figures 7, 8, 9 and 10, respectively. The intense broad bands in the region

3300-3450 cm^{-1} in the spectra of chitosan and chitosan-linked 1-hydroxy-2-pyridinethione-4-carboxylic acid resin are attributed to the intramolecular hydrogen bonded O-H stretching vibration which appears superimposed with N-H stretching bands.

The absorption bands observed in the IR spectrum of 1-hydroxy-2-pyridinethione-4-carboxylic acid in the region of 3085 cm^{-1} are attributed to the aromatic C-H stretching vibrations, while those between 2885-2946 cm^{-1} are due to the stretching vibrations of the aliphatic C-H stretching vibrations. The carbonyl stretching vibration at 1713 cm^{-1} in the spectrum of 1-hydroxy-pyridinethione-4-carboxylic acid has disappeared and a shoulder around 1630 cm^{-1} has appeared instead in the spectrum of the chitosan-linked 1-hydroxy-pyridinethione-4-carboxylic acid due to the formation of amide bond. Several bands appear in the spectrum of 1-hydroxy-pyridinethione-4-carboxylic acid in the region 1100–1600 cm^{-1} which are attributed to the O-N-C-S group and ring C=C stretching vibration of 1-hydrox 2-pyridinethione; some of these bands appear in the spectrum of chitosan-linked 1-hydroxy-pyridinethione-4-carboxylic acid resin at 1460 cm^{-1}, around 1400 cm^{-1}, and at 1291 cm^{-1}. Other bands seem to be superimposed with strong bands of chitosan in the regions 1000 -1115 cm^{-1} and 1500 -1600 cm-1.

The IR spectra of the chitosan-linked 1-hydroxy-2-pyridinethione-4-carboxylic acid loaded with lead(II) and copper(II) ions are shown in Figures 11 and 12. The spectra are similar and resemble the spectrum of the chitosan-linked 1-hydroxy-pyridinethione-4-carboxylic acid resin. Some bands change positions especially in the region1000 – 1100 cm^{-1} probably due to the changes in C-S stretching frequency which is expected in that region. The C-S stretching frequency appears at 1135 cm^{-1} in the spectrum of 1-hydroxy-2-pyridinethione and is shifted to 1085 cm^{-1} in its lead complex (Abu-Dari, K.-1988). Similar results were reported earlier for 1-hydroxy-2-pyridinethione ligands and

their lead and other metal complexes (Abu-Dari, K.-1988; Abu-Dari, K.-1991, and Abu-Dari, K.-1993).

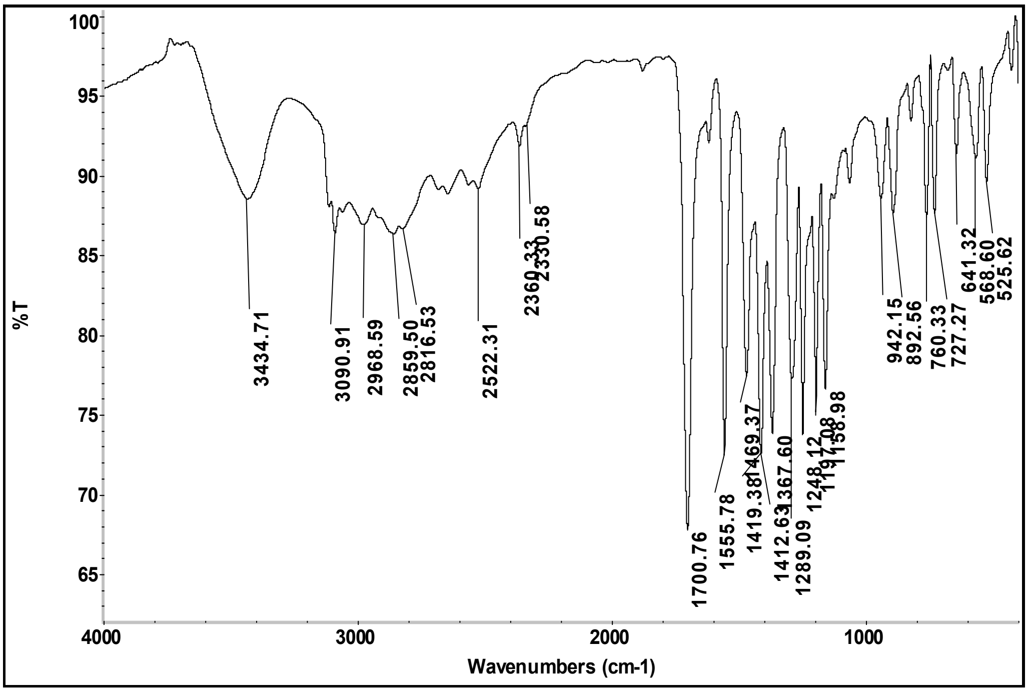


Figure 6. IR spectrum of 1-Hydroxy-pyridine thione-4-carboxylic acid

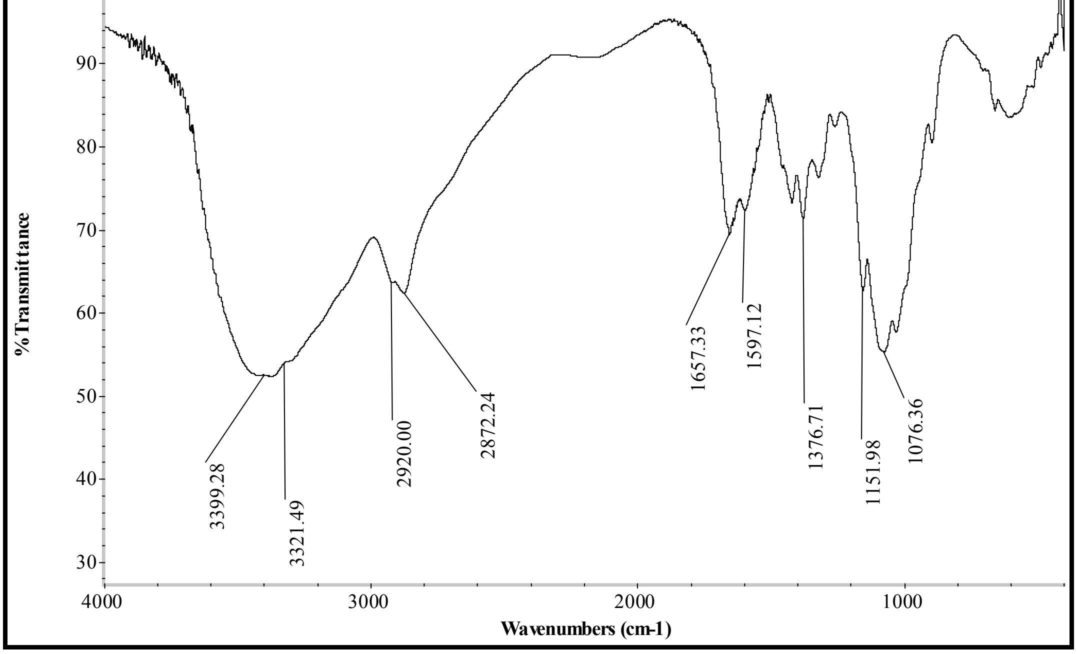


Figure 7. IR spectrum of chitosan

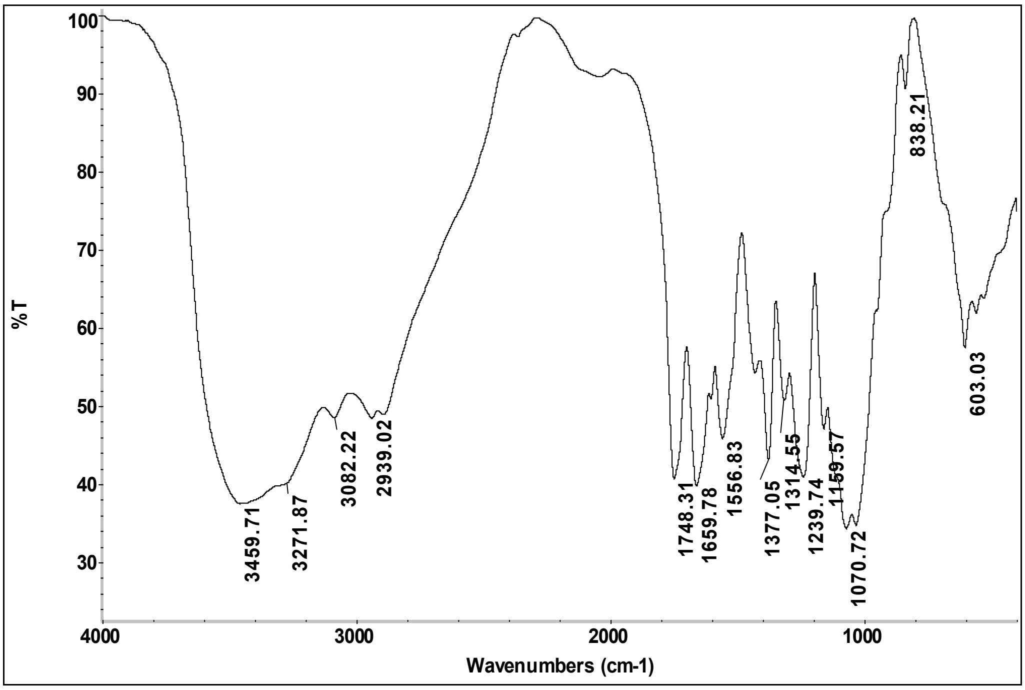


Figure 8. IR spectrum of acetylated chitosan

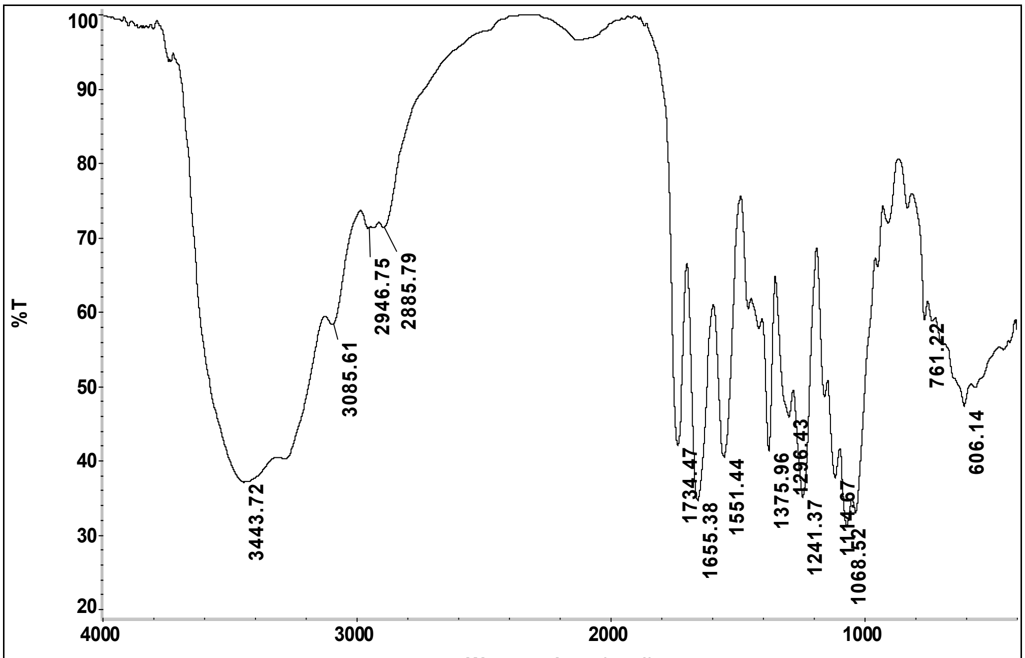


Figure 9. IR spectrum of chitosan-linked 1-hydroxy-2-pyridinethione-4-carboxylic acid (resin).

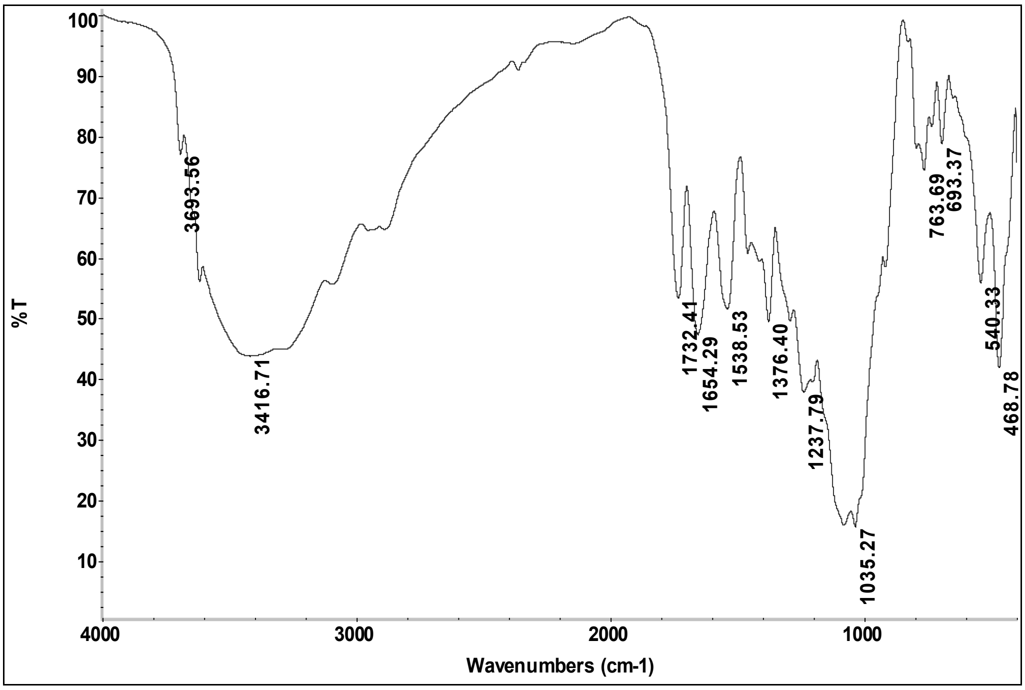


Figure 10. IR spectrum of resin loaded with lead(II)

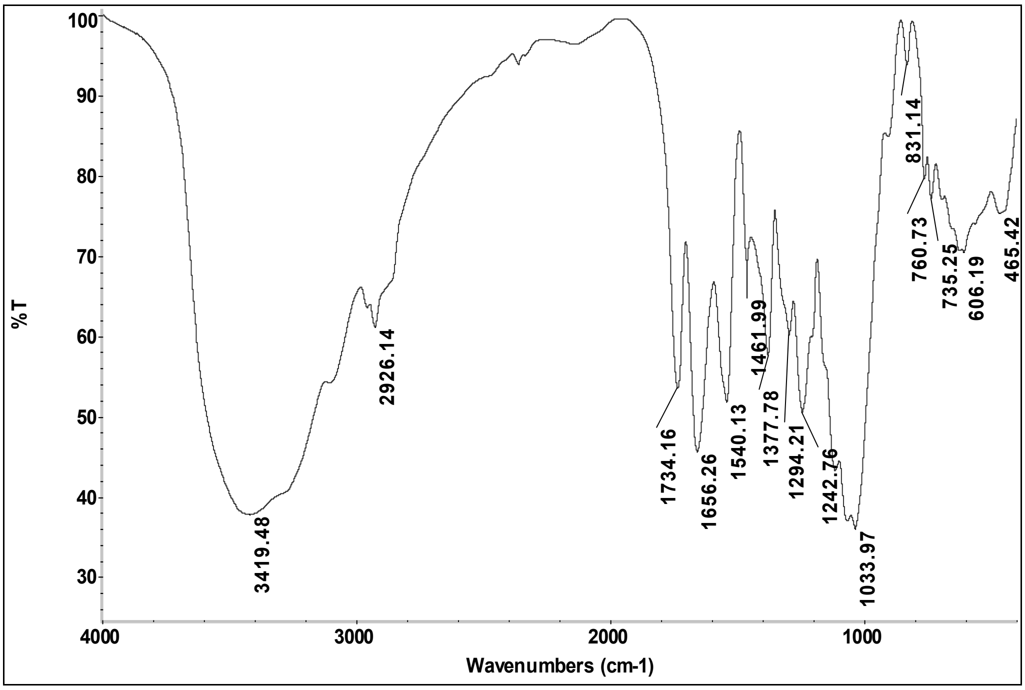


Figure 11. IR spectrum of resin loaded with cupper(II)

3.1.2.4 Thermal analysis techniques

Two thermal techniques were used for the characterization of polymers which are Differential Scanning Calorimetery (DSC) and Thermogravimetric Analysis (TGA).

In DSC the differences in heat flow in a substance and a reference are measured as a function of sample temperature. The DSC thermograms for chitosan, acetylated chitosan and resin were recorded in nitrogen and are shown in Figures 16-18, respectively**.** The TGA and DTG (Differential Thermogravimetric) thermograms for chitosan, acetylated chitosan and resin were also recorded in nitrogen and are shown in Figures 13 – 15, respectively. In TGA the mass of sample in a controlled atmosphere is recorded as a function of temperature, to get thermogram or thermal decomposition curve (Skoog, et al., 1998). TG and DTG curves shown represent the main stages of mass loss for chitosan, acetylated chitosan, and resin. TG curves reveal two main stages of weight loss (%) observed for the chitosan, acetylated chitosan and resin. The first peak represents solvent peak, appears around 100 °C in chitosan and it originates from the evaporation of the water contained in the chitosan itself; due to dehydration. In the acetylated chitosan and resin this solvent peak occurs at lower temperatures probably due to a lower packing order that results from bulky pendent groups.

The second stage of the weight loss is attributed to the thermal degradation of the corresponding polymer; it gave exothermic peaks in the DSC curves. Chitosan shows this peak at approximately 305.0 °C, with a 32.18% loss in polymer mass. Aceytelated chitosan undergoes mass loss at about 207.5 °C, with also 19.84% weight loss. Resin undergoes a mass loss at a temperature 242.2 °C with 17.76% loss. During the degradation of these polymers, it is obvious that their degradation temperatures are less than that for pure chitosan which indicates that the degredation of acetylated chitosan

and resin will be at lower temperature and this will reduce temperature of biodegradability which is a good advantage comared with chitosan (Justi et al., 2004).

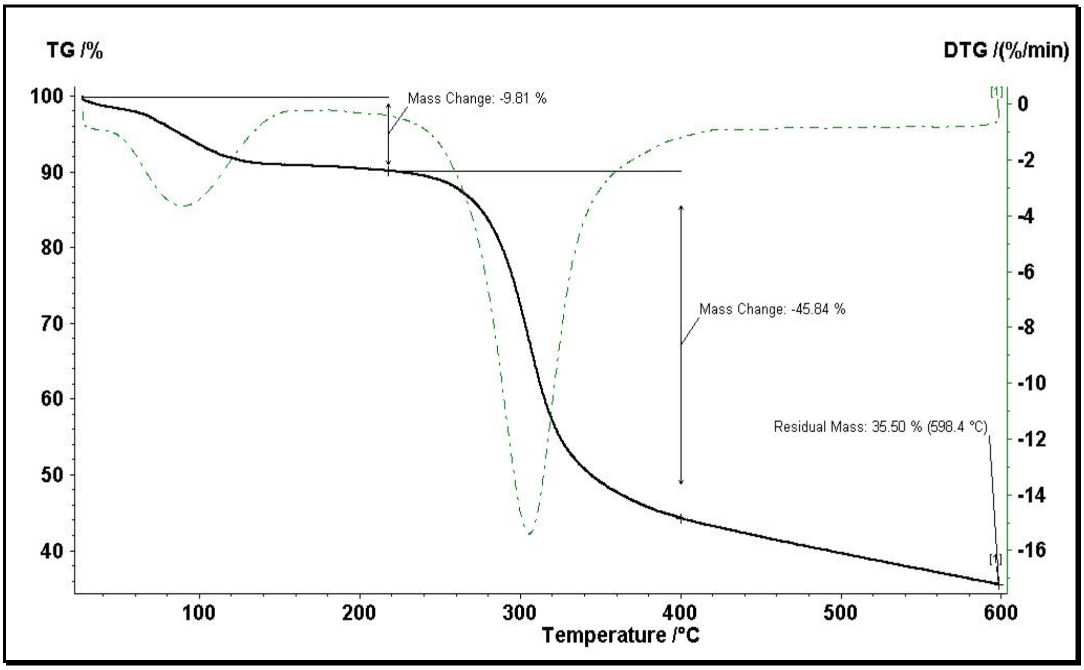


Figure 12. TGA thermogram of chitosan.

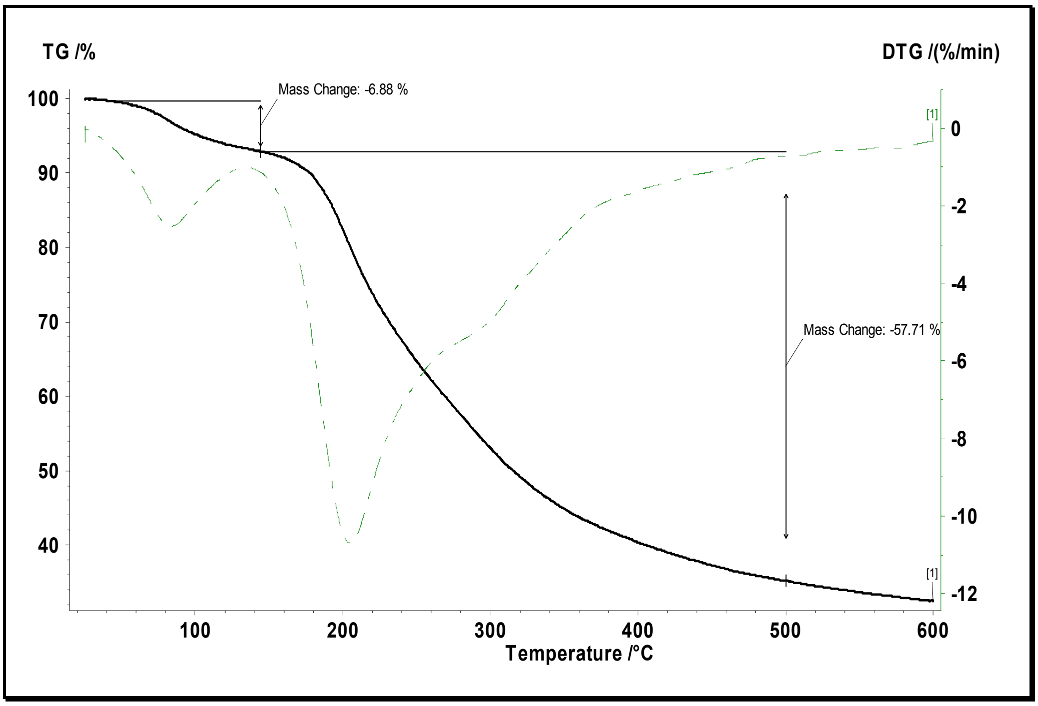


Figure 13. TGA thermogram of acetylated chitosan.

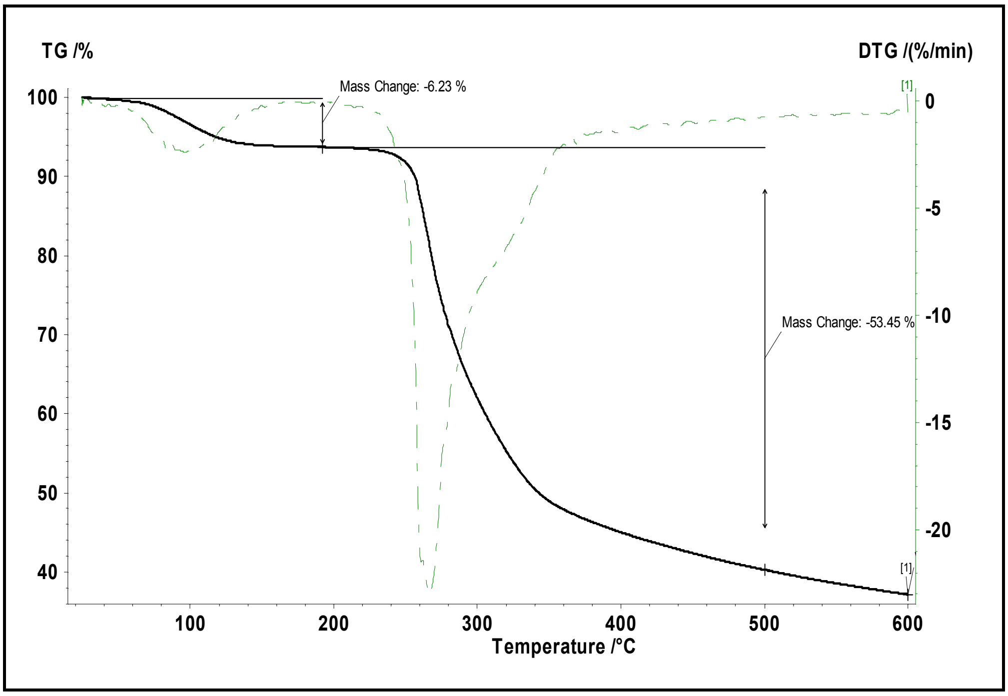


Figure 14. TGA thermogram of resin

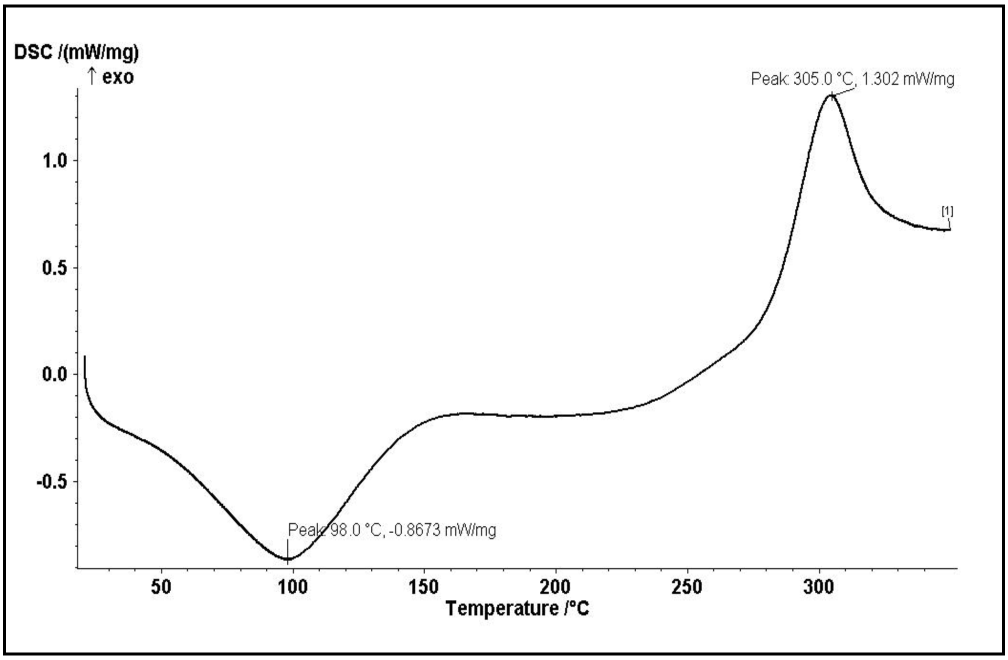


Figure 15. DSC thermogram of chitosan

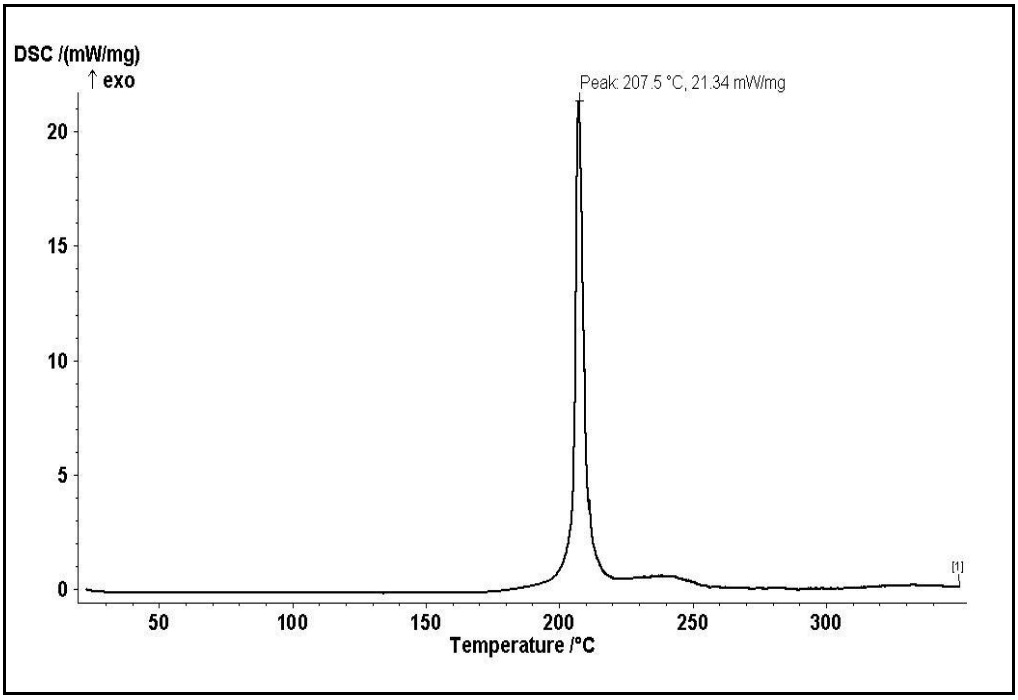


Figure 16. DSC thermogram of acetylated chitosan.

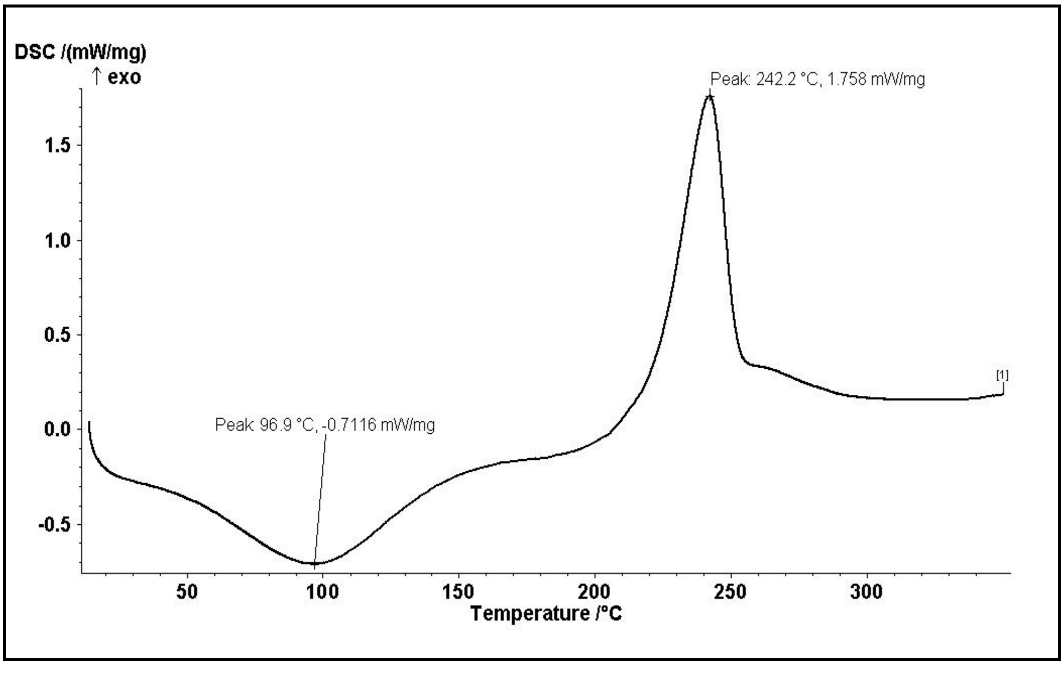


Figure 17. DSC thermogram of resin.

3.2 Sample blank

No appreciable change in lead concentration was observed 548.2 ppm and 526.7 ppm for direct measuring and after 24 hrs measuring respectively.

Result showed that no lead hydroxide has been precipitated.

3.3 Isothermal behavior of the polymers

3.3.1 Adsorption study of Pb(II)

Batch adsorption experiments were used to study the isothermal behavior of the resin towards Pb(II), The large and small particle-size resin in 25.0 mL of buffer solution at pH = 7.0 were equilibrated for 2 hours. Samples of 25 mL of lead(II) solutions of different concentrations ranging from 40-1000 ppm were added to produce a total volume of 50 mL solutions containing 2.0-25.0 mg of metal ion. The mixtures were shaken for 12 hours at different temperatures of 15.0 °C, 25.0 °C, and 35.0 °C. The results are presented in Tables 4-15 for the large and small particle-size resin. The plot of adsorption isotherms together with Freundlich and Langmuir Linearized models at each temperature for the large and small particle-size resin are given in Figures 20, 21, 23, and 24.

Figures 19 and 22 show the quantity of Pb(II) ions adsorbed at the surface of the corresponding resin and the concentration of Pb(II) ions in the aqueous phase at equilibrium. These relationships between q and C show that the adsorption capacity increases with the increase of equilibrium concentration of the metal ion in the aqueous phase, progressively reaching Pb(II) saturation at higher concentrations. It is also obvious that the isotherm shifts up with increasing temperature, and that the small-particle-size resin has good capacity than the large-particle resin to adsorb Pb(II) due to high surface area.

Table 4. Pb(II) uptake by resin as a function of Pb(II) concentration at pH =7.0, temperature = 15 °C, total volume of solution = 50.0 mL of Pb(II) and 0.1000 g of the large particle-size resin

Initial Concentration of Pb(II) (ppm)	Equilibrium Concentration of Pb(II) in Solution (ppm)	Concentration Adsorbed of Pb(II) (ppm)	% Uptake
10.00	2.895	7.108	71.08
40.00	25.20	14.80	37.00
50.00	31.70	18.30	36.60
100.0	65.80	34.20	34.20
150.0	101.4	48.60	32.40
200.0	137.2	62.80	31.40
250.0	182.2	67.80	27.12
300.0	219.2	80.80	26.93
350.0	257.9	92.10	26.31
400.0	302.0	98.00	24.50
450.0	344.8	105.2	23.38
500.0	396.4	103.6	20.72

Table 5. Results for concentration variation isotherm for adsorption of Pb(II) on resin at pH = 7.0 , temperature = 15 °C, with total volume of solution = 50.0 mL of Pb(II) and 0.1000 g of the large particle-size resin

q (mg Pb(II) adsorbed per g polymer)	C (mg Pb(II)/L in solution)	C/q (g/L)	Log q	Log C
1.921	2.895	2.813	0.585	0.461
7.400	25.20	3.405	0.869	1.401
9.150	31.70	3.464	0.961	1.501
17.10	65.80	3.848	1.232	1.818
24.30	101.4	4.173	1.385	2.006
31.40	137.2	4.369	1.496	2.137
33.90	182.2	5.375	1.530	2.261
40.40	219.2	5.426	1.606	2.341
46.05	257.9	5.600	1.663	2.411
49.00	302.0	6.163	1.690	2.480
52.60	344.8	6.555	1.721	2.537
51.80	396.4	7.653	1.714	2.598

Table 6. Pb(II) uptake by resin as a function of Pb(II) concentration at pH = 7.0, temperature = 25 °C, total volume of solution = 50.0 mL of Pb(II) and 0.1000 g of the large particle-size resin

Initial Concentration of Pb(II) (ppm)	Equilibrium Concentration of Pb(II) in Solution (ppm)	Concentration Adsorbed of Pb(II) (ppm)	% Uptake
10.00	2.311	7.689	76.89
40.0	18.10	21.90	54.75
50.0	25.00	25.00	50.00
100.0	54.60	45.40	45.40
150.0	89.00	61.00	40.67
200.0	120.7	79.30	39.65
250.0	162.5	87.50	35.00
300.0	197.3	102.7	34.23
350.0	238.1	111.9	31.97
400.0	286.2	113.8	28.45
450.0	326.9	123.1	27.36
500.0	371.8	128.2	25.64

Table 7. Results for concentration variation isotherm for adsorption of Pb(II) on resin at pH = 7.0, temperature = 25 °C, with total volume of solution = 50.0 mL of Pb(II) and 0.1000 g of the large particle-size resin

q (mg Pb(II) adsorbed per g polymer)	C (mg Pb(II)/L in solution)	C/q (g/L)	Log q	Log C
3.844	2.311	0.601	0.584	0.363
10.95	18.10	1.653	1.039	1.257
12.50	25.00	2.000	1.097	1.398
22.70	54.60	2.405	1.356	1.737
30.50	89.00	2.918	1.484	1.949
39.65	120.7	3.044	1.598	2.082
43.75	162.5	3.714	1.641	2.211
51.35	197.3	3.842	1.711	2.295
55.95	238.1	4.256	1.748	2.377
56.90	286.2	5.029	1.755	2.456
61.55	326.9	5.311	1.789	2.514
64.10	371.8	5.800	1.806	2.570

Table 8. Pb(II) uptake by resin as a function of Pb(II) concentration at pH = 7.0, temperature = 35 °C, total volume of solution = 50.0 mL of Pb(II) and 0.1000 g of the large particle-size resin

Initial Concentration of Pb(II) (ppm)	Equilibrium Concentration of Pb(II) in Solution (ppm)	Concentration Adsorbed of Pb(II) (ppm)	% Uptake
10.00	2.184	7.816	77.25
40.00	15.10	24.90	62.25
50.00	21.30	28.70	57.40
100.0	47.20	52.80	52.80
150.0	77.20	72.80	48.53
200.0	105.0	95.00	47.50
250.0	149.8	100.2	40.08
300.0	183.2	116.8	38.93
350.0	223.2	126.8	36.29
400.0	271.5	128.5	32.13
450.0	311.7	138.3	30.73
500.0	354.1	145.9	29.18

Table 9. Results for concentration variation isotherm for adsorption of Pb(II) on polymer I at pH = 7.0 , temperature = 35 °C, with total volume of solution = 50.0 mL of Pb(II) and 0.1000 g of the large particle-size resin.

q (mg Pb(II) adsorbed per g polymer)	C (mg Pb(II)/L in solution)	C/q (g/L)	Log q	Log C
3.908	2.184	0.558	0.592	0.339
12.45	15.10	1.213	1.188	0.959
14.35	21.30	1.484	1.263	1.124
26.40	47.20	1.787	1.530	1.507
36.40	77.20	2.121	1.666	1.757
47.50	105.0	2.211	1.759	1.929
50.10	149.8	2.990	1.810	2.082
58.40	183.2	3.137	1.862	2.188
63.40	223.2	3.521	1.891	2.289
64.25	271.5	4.226	1.907	2.377
69.15	311.7	4.508	1.925	2.449
72.95	354.1	4.854	1.951	2.506

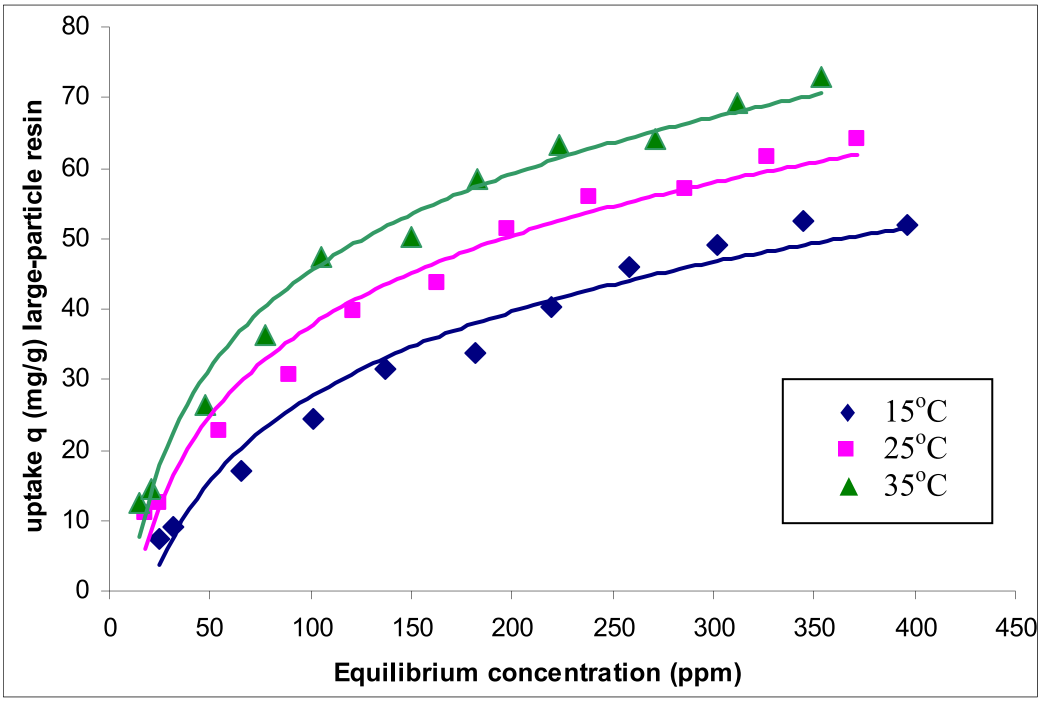


Figure 18. Adsorption isotherms of Pb(II) by large-particle resin at different temperatures of 15 °C, 25 °C and 35 °C. The curves represent the fitted logarithmic curves for adsorption at each temperature.

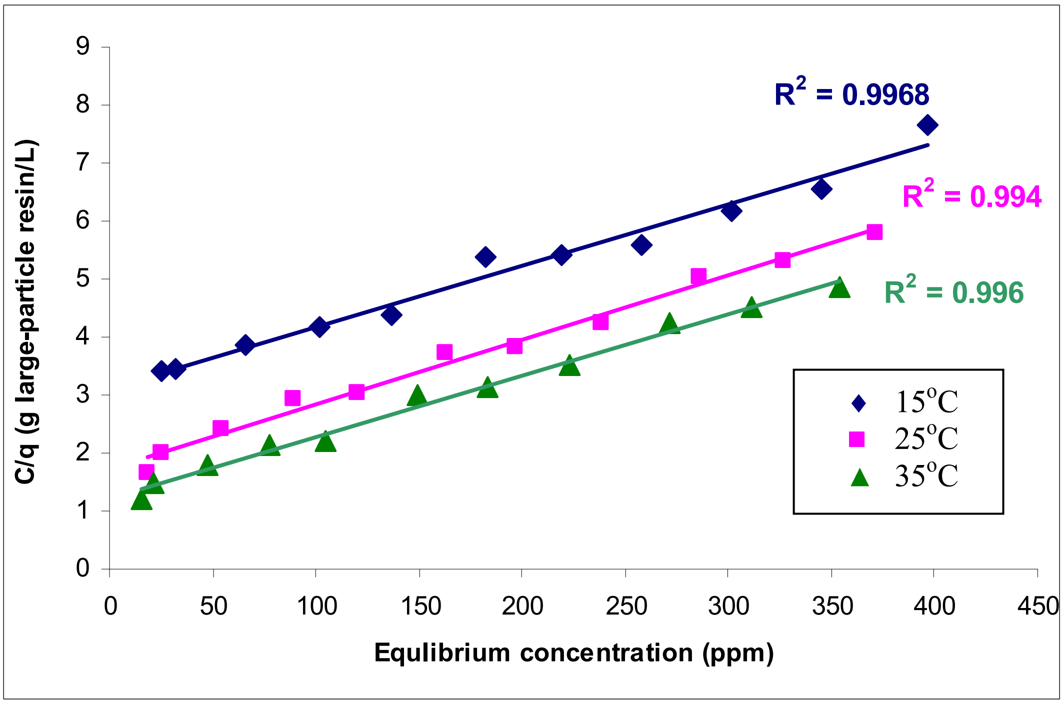


Figure 19. Linearized Langmuir-form (III) for Pb(II) adsorption by large-particle resin at different temperatures of 15 °C, 25 °C and 35 °C. The lines represent the fitted linear equations at each temperature.

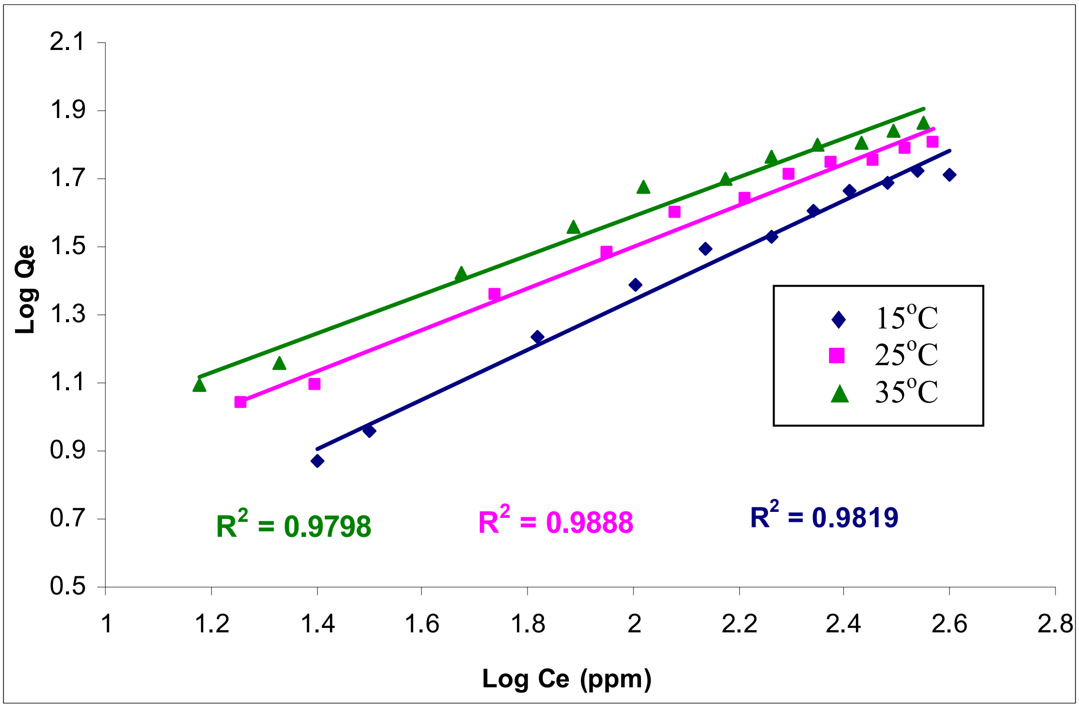


Figure 20. Linearized Freundlich for Pb(II) adsorption by large-particle resin at different temperatures of 15 °C, 25 °C and 35 °C. The lines represent the fitted linear equations at each temperature.

Table 10. Pb(II) uptake by resin as a function of Pb(II) concentration at pH = 7.0, temperature = 15 °C, total volume of solution = 50.0 mL of Pb(II) and 0.1000 g of the small-particle resin

Initial Concentration of Pb(II) (ppm)	Equilibrium Concentration of Pb(II) in Solution (ppm)	Concentration Adsorbed of Pb(II) (ppm)	% Uptake
10.00	1.215	8.785	87.85
40.00	5.400	34.60	86.50
50.00	10.30	39.70	79.40
100.0	21.20	78.80	78.80
150.0	50.90	99.10	66.06
200.0	80.90	119.1	59.55
250.0	110.3	139.7	55.88
300.0	145.6	154.4	51.47
350.0	185.7	164.3	46.94
400.0	215.4	184.6	46.15
450.0	258.8	191.2	42.49

Table 11. Results for concentration variation isotherm for adsorption of Pb(II) on resin at pH = 7.0 and temperature = 15 °C, with total volume of solution = 50.0 mL of Pb(II) and 0.1000 g of the small-particle resin.

q (mg Pb(II) adsorbed per g polymer)	C (mg Pb(II)/L in solution)	C/q (g/L)	Log q	Log C
4.392	1.215	0.276	0.344	-0.237
17.30	5.400	0.312	1.238	0.733
19.85	10.30	0.518	1.297	1.013
39.40	21.20	0.538	1.595	1.326
49.55	50.90	1.027	1.695	1.706
59.55	80.90	1.358	1.775	1.908
69.85	110.3	1.579	1.844	2.045
77.20	145.6	1.886	1.887	2.163
82.15	185.7	2.260	1.915	2.268
92.30	215.4	2.334	1.965	2.333
95.60	258.8	2.707	1.980	2.413
98.40	303.2	3.081	1.993	2.482

Table 12. Pb(II) uptake by resin as a function of Pb(II) concentration at pH = 7.0, temperature = 25 °C, total volume of solution = 50.0 mL of Pb(II) and 0.1000 g of the small-particle resin

Initial Concentration of Pb(II) (ppm)	Equilibrium Concentration of Pb(II) in Solution (ppm)	Concentration Adsorbed of Pb(II) (ppm)	% Uptake
10.00	0.289	9.711	97.11
40.00	1.700	38.30	95.75
50.00	5.300	44.70	89.40
100.0	12.50	87.50	87.50
150.0	30.60	119.4	79.60
200.0	60.20	139.8	69.90
250.0	80.70	169.3	67.72
300.0	125.8	174.2	58.07
350.0	166.8	183.2	52.34
400.0	202.8	197.2	49.30
450.0	246.5	203.5	45.22
500.0	280.6	219.4	43.88

Table 13. Results for concentration variation isotherm for adsorption of Pb(II) on resin at pH = 7.0, temperature = 25 °C, with total volume of solution = 50.0 mL of Pb(II) and 0.1000 g of the small-particle resin

q (mg Pb(II) adsorbed per g polymer)	C (mg Pb(II)/L in solution)	C/q (g/L)	Log q	Log C
4.855	0.289	97.11	0.686	-0.539
19.15	1.700	0.088	1.282	0.230
22.35	5.300	0.237	1.349	0.724
43.75	12.50	0.285	1.641	1.096
59.70	30.60	0.513	1.776	1.485
69.90	60.20	0.861	1.844	1.779
84.65	80.70	0.953	1.927	1.906
87.10	125.8	1.444	1.941	2.099
91.60	166.8	1.821	1.962	2.222
98.60	202.8	2.056	1.994	2.307
101.7	246.5	2.423	2.007	2.391
109.7	280.6	2.557	2.040	2.448

Table 14. Pb(II) uptake by resin as a function of Pb(II) concentration at pH = 7.0, temperature = 35 °C, total volume of solution = 50.0 mL of Pb(II) and 0.1000 g of the small-particle resin

Initial Concentration of Pb(II) (ppm)	Equilibrium Concentration of Pb(II) in Solution (ppm)	Concentration Adsorbed of Pb(II) (ppm)	% Uptake
10.00	0.051	9.949	99.49
40.00	0.100	39.90	99.75
50.00	1.400	48.60	97.20
100.0	7.800	92.20	92.20
150.0	22.40	127.6	85.07
200.0	46.50	153.5	76.75
250.0	70.30	179.7	71.88
300.0	105.6	194.4	64.80
350.0	141.2	208.8	59.66
400.0	180.0	220.0	55.00
450.0	213.6	236.4	52.53
500.0	254.8	245.2	49.04

Table 15. Results for concentration variation isotherm for adsorption of Pb(II) on resin at pH = 7.0 , temperature = 35 °C, with total volume of solution = 50.0 mL of Pb(II) and 0.1000 g of the small-particle resin

q (mg Pb(II) adsorbed per g polymer)	C (mg Pb(II)/L in solution)	C/q (g/L)	Log q	Log C
4.974	0.051	0.004	-1.292	0.696
19.95	0.100	0.005	1.299	-1.000
24.30	1.400	0.057	1.385	0.146
46.10	7.800	0.169	1.664	0.892
63.80	22.40	0.351	1.805	1.350
76.75	46.50	0.605	1.885	1.667
89.85	70.30	0.782	1.953	1.847
97.20	105.6	1.086	1.987	2.024
104.4	141.2	1.352	2.018	2.149
110.0	180.0	1.636	2.041	2.255
118.2	213.6	1.807	2.073	2.329
122.6	254.8	2.078	2.088	2.406

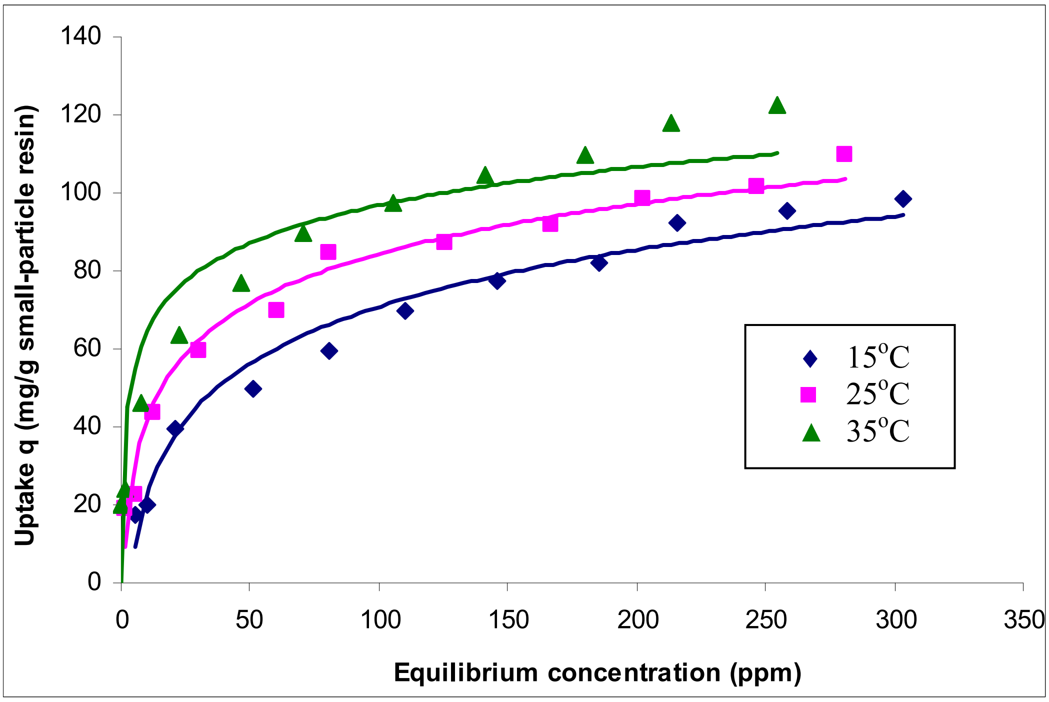


Figure 21. Adsorption isotherms of Pb(II) by small particle resin at different temperatures of 15 °C, 25 °C and 35 °C. The lines represent the fitted logarithmic curves for adsorption at each temperature.

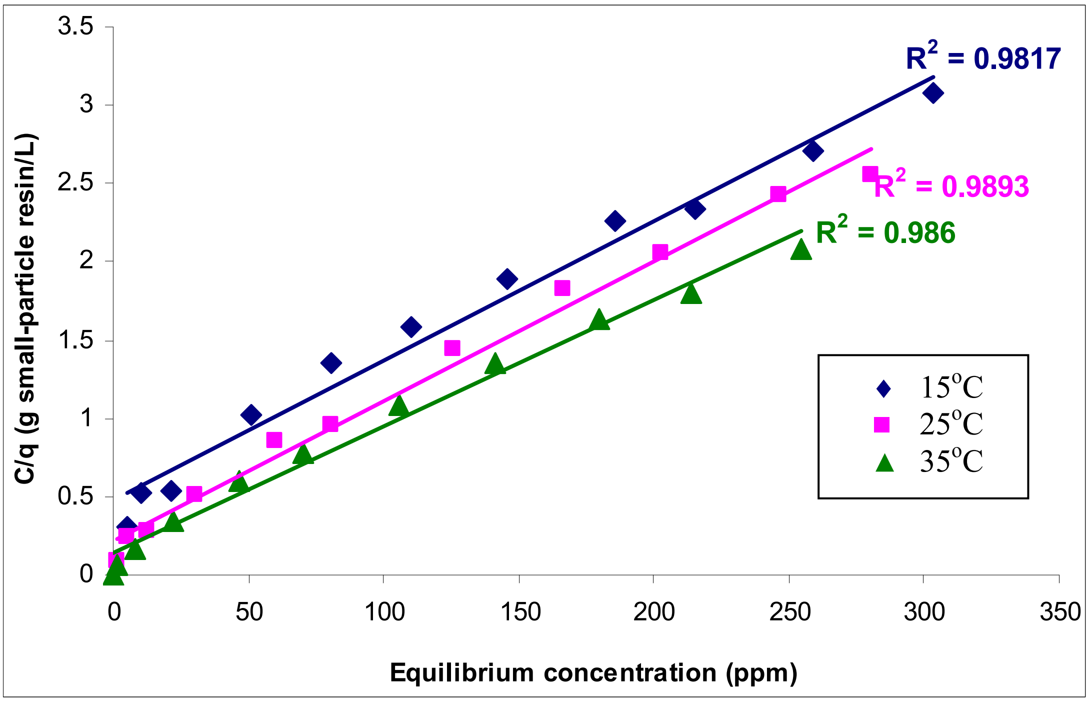


Figure 22. Linearized Langmuir- form (III) for Pb(II) adsorption by small-particle resin at different temperatures of 15 °C, 25 °C and 35 °C. The lines represent the fitted linear equations at each temperature.

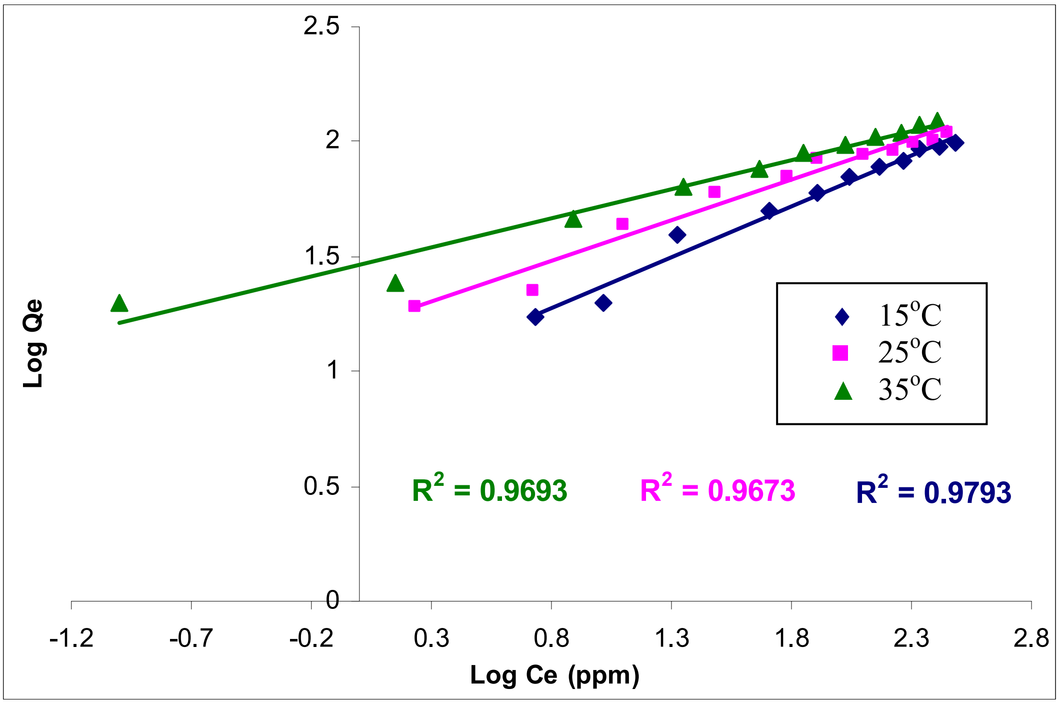


Figure 23. Linearized Freundlich for Pb(II) adsorption by small-particle resin at different temperatures of 15 °C, 25 °C and 35 °C. The lines represent the fitted linear equations at each temperature.

3.3.2 Langmuir behavior

Experimental data showed a good agreement with Langmuir model for Pb(II) adsorption by large and small particle resins at pH = 7.0. The plots of C/q versus C (Equation 2) are suitable for determining the adsorption parameters q_m and K_L. Linearity of this plot for resins of large and small particles indicate the presence of homogenous surface site of interaction. The linear form with correlation coefficients (R^2) greater than 0.99 for large-particle resin and greater than 0.98 for small-particle resin were obtained for the large and small particles resin at different temperatures of 15 °C, 25 °C and 35 °C are shown in Figures 20 and 23. The monolayer adsorption capacity q_m and the Langmuir constant K_L of adsorption isotherms are given in Tables 16 and 17.

3.3.3 Freundlich behavior

A plot of log q versus log c (Equation 4) gives a straight line with an intercept equals log K_F and a slope of β when the Freundlich relation holds, where K_F is roughly an indicator of the adsorption capacity and β (1/n) is the adsorption intensity. This relationship is well applicable for the large and small-particle resins where linear curves with correlation coefficients (R^2) greater than 0.97 for large-particle resin and greater than 0.96 for small-particle resin were obtained as shown before in Figures 21 and 24 indicating that the average energy of adsorption decreases with increasing adsorption density.

Tables 16 and 17 list the calculated results. The magnitude of β (1/n) gives an indication of the favorability of adsorption; values of $n > 1$ represent favorable adsorption condition (McKay, 1982). Thus, from these values it is inferred that the Pb(II) adsorption process by the small-particle resin is more favorable than large-particle resin.

3.3.4 Effect of temperature

From the linearized Langmuir and Freundlich isotherms, the calculated isothermal parameters presented in Tables 16 and 17 are found to correlate with the temperature as follows: q_m, the monolayer adsorption capacity is directly proportional to the temperature of the polymer. This increase in adsorption capacity with temperature suggests that the active surface sites available for adsorption increase with temperature. In addition, this increase may be attributed to the change in pore size which enhances rate of intraparticle diffusion of solute.

The Langmuir K_L values and the Freundlich K_F values isothermal constants, are directly proportional to the temperature of the polymer, this indicates that the adsorption capacity increases with increasing temperature as a result of the higher interaction energy at higher temperatures. Moreover, the value of the constant n was always more than unity which indicates a favorable adsorption process.

From Tables 16 and 17 we can see that the adsorption capacity of small-particle resin is much higher than that of large-particle resin.

Table 16. Calculated values of Langmuir and Freundlich isothermal constants from the adsorption of Pb(II) by large-particle resin at 15 °C, 25 °C and 35 °C

Large-particle resin							
Temp. (°C)	Q_e (mg/g)	K_L (L/mg)	R^2	β	N	K_F (mg^{1-N} g^{-1} L^N)	R^2
15 °C	69.30	0.006	0.997	0.647	1.545	1.764	0.982
25 °C	81.60	0.011	0.994	0.540	1.851	3.855	0.986
35 °C	89.45	0.015	0.996	0.499	2.004	5.557	0.979

Table 17. Calculated values of Langmuir and Freundlich isothermal constants from the adsorption of Pb(II) by small-particle resin at 15 °C, 25 °C and 35 °C

Small-particle resin							
Small resin	Qe (mg/g)	K_L (L/mg)	R^2	β	N	K_F ($mg^{1-N} g^{-1} L^N$)	R^2
15 °C	98.40	0.019	0.982	0.444	2.251	8.330	0.979
25 °C	105.2	0.043	0.993	0.350	2.854	15.82	0.965
35 °C	122.6	1.174	0.986	0.253	3.942	29.24	0.969

3.4 Chelation characteristics of the polymers

Two methods are commonly employed for investigating the sorption characteristics of chelating resins; the dynamic and the static methods. Dynamic methods are applied by passing a known volume of known metal ion concentration, at constant flow rate through a column which contains a preconditioned chelating resin. In the static method, a known amount of the resin is equilibrated in a known concentration of metal ion under continuous shaking for a definite period of time. The metal-ion uptake is then determined by (AAS). Moreover, the chelation capacity and selectivity of chelating polymers are normally discussed in terms of the distribution coefficient (K_d).

3.4.1 Metal uptake by chitosan as function of contact time

The rate of interaction of the divalent metal ions with chitosan and resin were investigated by a batch equilibration technique. A Suspension of 0.1000 g of the dry resin was equilibrated for 2 hours with 25.0 mL buffer solution of pH = 7.0. An amount of 25.0 mL of 500 ppm ionic Pb(II), Cu(II), Zn(II), Ni(II) and Cd(II) solution were

added at 25 °C under continuous shaking for a definite period of time ranging from 0.08 to 24 hours.

Results are given in Tables 18-22 and in Figure 25 for chitosan, in Tables 23, 25, 27, 28 and 29 and in Figure 26 for large-particle resin and in Tables 24 and 26 for small-particle resin for Pb(II) and Cu(II), and in Figure 27 comparison between the uptake by large and small particle resin of Pb(II).

The curves show that the time needed to reach equilibrium is about 12 hour. The Pb(II), Cu(II), Zn(II), Ni(II) and Cd(II) adsorption by chitosan and resin is rapid at the beginning and **a**bout 50% of metal-ion uptake was achieved at the end of the twelve hour and thereafter it remains constant (plateau). At this equilibrium time, the percent uptake of Pb(II), Cu(II), Zn(III) and Ni(II) and Cd(II) by chitosan were 3.02%, 47.96%, 30.73%, 18.51% and 45.84% respectively. In constrat, the percent uptake of Pb(II), Cu(II), Zn(III) and Ni(II) and Cd(II) by large- particle resin were 25.40%, 22.68%, 17.00%, 12.06% and 11.00% respectively, and the percent uptake of Pb(II), Cu(II) by small particle resin were 47.68%, 23.58% respectively. The resin, with hard (oxygen) and soft (sulfur) donor species, aided in selectivity of soft lead ion. The use of small-particle resin with Pb(II) give high capacity due to their high surface areas and filtration capacity but no change in results for large and small resin with hard Cu(II).

Table 18. Lead(II) uptake by chitosan as function of contact time. Temperature = 25 ^{o}C, pH = 7.0 with total ionic strength of 0.10 M. Volume of solution = 50.0 mL containing 25.0 mg Pb(II) and 0.1000 g of the chitosan

Contact Time (hr)	Equilibrium Concentration of Pb(II) in solution (ppm)	Concentration of Pb(II) adsorbed(ppm)	Pb(II) uptake (mg/g)	% Uptake
0.08	500.0	0.000	0.000	0.000
0.25	496.0	3.980	1.990	0.790
0.50	494.9	5.060	2.530	1.010
1.00	492.5	7.500	3.750	1.500
3.00	484.8	15.12	7.560	3.020
6.00	477.5	22.50	11.25	4.500
12.00	474.9	25.06	12.53	5.010

Table 19. Copper(II) uptake by chitosan as a function of contact time. Temperature = 25 ^{o}C, pH = 7.0 with total ionic strength of 0.10 M. Volume of solution = 50.0 mL containing 25.0 mg Cu(II) and 0.1000 g of the chitosan

Contact Time (hr)	Equilibrium Concentration of Cu(II) in solution (ppm)	Concentration of Cu(II) adsorbed(ppm)	Cu(II) uptake (mg/g)	% Uptake
0.08	448.7	51.26	25.63	10.25
0.25	425.1	74.90	37.45	14.98
0.50	400.8	99.12	49.56	19.824
1.00	356.6	143.40	71.70	28.68
3.00	299.0	201.0	100.5	40.20
6.00	277.0	223.0	111.5	44.60
12.00	268.6	231.4	115.7	46.28
24.00	260.2	239.8	119.9	47.96

Table 20. Zinc(II) uptake by chitosan as a function of contact time. Temperature = 25 ^{o}C, pH = 7.0 with total ionic strength of 0.10 M. Volume of solution = 50.0 mL containing 25.0 mg ZnII) and 0.1000 g of the chitosan

Contact Time (hr)	Equilibrium Concentration of Zn(II) in solution (ppm)	Concentration of Zn(II) adsorbed(ppm)	Zn(II) uptake (mg/g)	% Uptake
0.08	462.5	37.54	18.77	7.510
0.25	455.4	44.60	22.30	8.920
0.50	453.7	46.30	23.15	9.260
1.00	444.5	55.46	27.73	11.09
3.00	382.6	117.4	58.70	23.48
6.00	380.3	119.7	59.85	23.94
12.00	377.7	122.2	61.12	24.45
24.00	346.3	153.7	76.83	30.73

Table 21. Nickel(II) uptake by chitosan as a function of contact time. Temperature = 25 ^{o}C, pH = 7.0 with total ionic strength of 0.10 M. Volume of solution = 50.0 mL containing 25.0 mg Ni(II) and 0.1000 g of the chitosan

Contact Time (hr)	Equilibrium Concentration of Ni(II) in solution (ppm)	Concentration of Ni(II) adsorbed(ppm)	Ni(II) uptake (mg/g)	% Uptake
0.08	460.1	39.90	19.95	7.980
0.25	456.1	43.94	21.97	8.790
0.50	452.9	47.10	23.55	9.420
1.00	449.7	50.34	25.17	10.07
3.00	441.5	58.50	29.25	11.70
6.00	419.5	80.46	40.23	16.09
12.00	417.4	82.64	41.32	16.53
24.00	407.5	92.54	46.27	18.51

Table 22. Cadmium(II) uptake by chitosan as a function of contact time. Temperature = 25 °C, pH = 7.0 with total ionic strength of 0.10 M. Volume of solution = 50.0 mL containing 25.0 mg Cd(II) and 0.1000 g of the chitosan

Contact Time (hr)	Equilibrium Concentration of Cd(II) in solution (ppm)	Concentration of Cd(II) adsorbed(ppm)	Cd(II) uptake (mg/g)	% Uptake
0.08	478.6	21.40	10.70	4.280
0.25	469.6	30.38	15.19	6.080
0.50	447.7	52.30	26.15	10.46
1.00	417.1	82.90	41.45	16.58
3.00	365.7	134.3	67.15	26.86
6.00	310.6	189.4	94.72	37.89
12.00	281.4	218.6	109.3	43.72
24.00	270.8	229.2	114.6	45.84

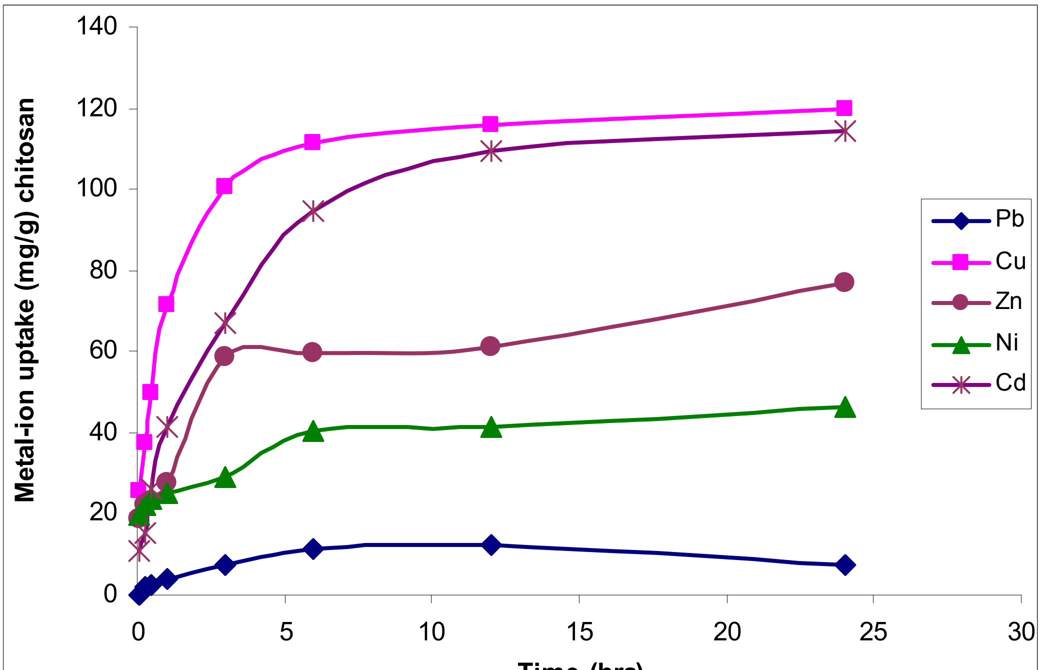


Figure 24. Pb(II), Cu(II), Zn(II), Ni(II), and Cd(II) uptake by chitosan as a function of contact time.

Table 23. Lead(II) uptake by resin as a function of contact time. Temperature = 25 ^{o}C, pH = 7.0 with total ionic strength of 0.10 M. Volume of solution = 50.0 mL containing 25.0 mg Pb(II) and 0.1000 g of the large-particle resin

Contact Time (hr)	Equilibrium Concentration of Pb(II) in solution (ppm)	Concentration of Pb(II) adsorbed(ppm)	Pb(II) uptake (mg/g)	% Uptake
0.08	471.8	28.20	14.10	5.640
0.25	465.4	34.60	17.30	6.920
0.50	451.8	48.20	24.10	9.640
1.00	449.1	50.90	25.40	10.18
3.00	423.6	76.40	38.20	15.28
6.00	403.6	96.40	48.20	19.28
12.00	400.0	100.0	55.00	20.00
24.00	373.0	127.0	63.50	25.40

Table 24. Lead(II) uptake by resin as a function of contact time. Temperature = 25 ^{o}C, pH = 7.0 with total ionic strength of 0.10 M. Volume of solution = 50.0 mL containing 25.0 mg Pb(II) and 0.1000 g of the small-particle resin

Contact Time (hr)	Equilibrium Concentration of Pb(II) in solution (ppm)	Concentration of Pb(II) adsorbed(ppm)	Pb(II) uptake (mg/g)	% Uptake
0.08	354.2	145.8	72.92	29.17
0.25	342.5	157.5	78.75	31.50
0.50	327.5	172.5	86.25	34.50
1.00	325.8	174.2	87.09	34.84
3.00	314.2	185.8	92.92	37.17
6.00	282.5	217.5	108.7	43.50
12.00	276.4	223.6	111.8	44.72
24.00	261.6	238.4	119.2	47.68

Table 25. Copper(II) uptake by resin as a function of contact time. Temperature = 25 °C, pH = 7.0 with total ionic strength of 0.10 M. Volume of solution = 50.0 mL containing 25.0 mg Cu(II) and 0.1000 g of the large-particle resin

Contact Time (hr)	Equilibrium Concentration of Cu(II) in solution (ppm)	Concentration of Cu(II) adsorbed(ppm)	Cu(II) uptake (mg/g)	% Uptake
0.08	446.7	53.30	26.65	10.66
0.25	435.9	64.10	32.05	12.82
0.50	431.7	68.30	34.15	13.66
1.00	430.1	69.90	34.95	13.98
3.00	412.5	87.50	43.75	17.50
6.00	405.0	95.00	47.50	19.00
12.00	392.0	108.0	50.40	21.60
24.00	386.6	113.4	56.70	22.68

Table 26. Copper(II) uptake by resin as a function of contact time. Temperature = 25 °C, pH = 7.0 with total ionic strength of 0.10 M. Volume of solution = 50.0 mL containing 25.0 mg Cu(II) and 0.1000 g of the small particle resin.

Contact Time (hr)	Equilibrium Concentration of Cu(II) in solution (ppm)	Concentration of Cu(II) adsorbed(ppm)	Cu(II) uptake (mg/g)	% Uptake
0.08	421.9	78.06	39.03	15.61
0.25	418.7	81.30	40.65	16.26
0.50	415.4	84.60	42.30	16.92
1.00	414.3	85.70	42.85	17.14
3.00	412.7	87.30	43.65	17.46
6.00	402.1	97.90	48.95	19.58
12.00	397.6	102.4	51.20	20.48
24.00	382.1	117.9	58.95	23.58

Table 27. Zinc(II) uptake by resin as a function of contact time. Temperature = 25°C, pH = 7.0 with total ionic strength of 0.10 M. Volume of solution = 50.0 mL containing 25.0 mg Zn(II) and 0.1000 g of the small-particle resin

Contact Time (hr)	Equilibrium Concentration of Zn(II) in solution (ppm)	Concentration of Zn(II) adsorbed(ppm)	Zn(II) uptake (mg/g)	% Uptake
0.08	450.2	49.80	24.90	9.960
0.25	446.0	54.00	27.00	10.80
0.50	445.0	55.00	27.50	11.00
1.00	443.6	56.40	28.20	11.28
3.00	439.8	60.22	30.11	12.04
6.00	428.8	71.20	35.60	14.24
12.00	419.4	80.60	40.30	16.12
24.00	415.0	85.00	42.50	17.00

Table 28. Nickel(II) uptake by resin as a function of contact time. Temperature = 25°C, pH = 7.0 with total ionic strength of 0.10 M. Volume of solution = 50.0 mL containing 25.0 mg Ni(II) and 0.1000 g of the large particle resin

Contact Time (hr)	Equilibrium Concentration of Ni(II) in solution (ppm)	Concentration of Ni(II) adsorbed(ppm)	Ni(II) uptake (mg/g)	% Uptake
0.08	451.7	48.26	24.13	9.650
0.25	450.2	49.80	24.90	9.960
0.50	449.0	51.00	25.50	10.20
1.00	446.8	53.20	26.60	10.64
3.00	444.7	55.30	27.65	11.06
6.00	444.0	56.00	28.00	11.20
12.00	443.2	56.80	28.40	11.36
24.00	439.7	60.30	30.15	12.06

Table 29. Cadmium(II) uptake by acid resin as a function of contact time. Temperature = 25°C, pH = 7.0 with total ionic strength of 0.10 M. Volume of solution = 50.0 mL containing 25.0 mg Cd(II) and 0.1000 g of the large-particle resin

Contact Time (hr)	Equilibrium Concentration of Cd(II) in solution (ppm)	Concentration of Cd(II) adsorbed(ppm)	Cd(II) uptake (mg/g)	% Uptake
0.08	478.9	21.06	10.53	4.210
0.25	472.7	27.30	13.65	5.460
0.50	466.3	33.74	16.87	6.750
1.00	461.0	39.00	19.50	7.800
3.00	453.1	46.86	23.43	9.370
6.00	448.8	51.20	25.60	10.24
12.00	446.9	53.10	26.55	10.62
24.00	445.0	55.00	27.50	11.00

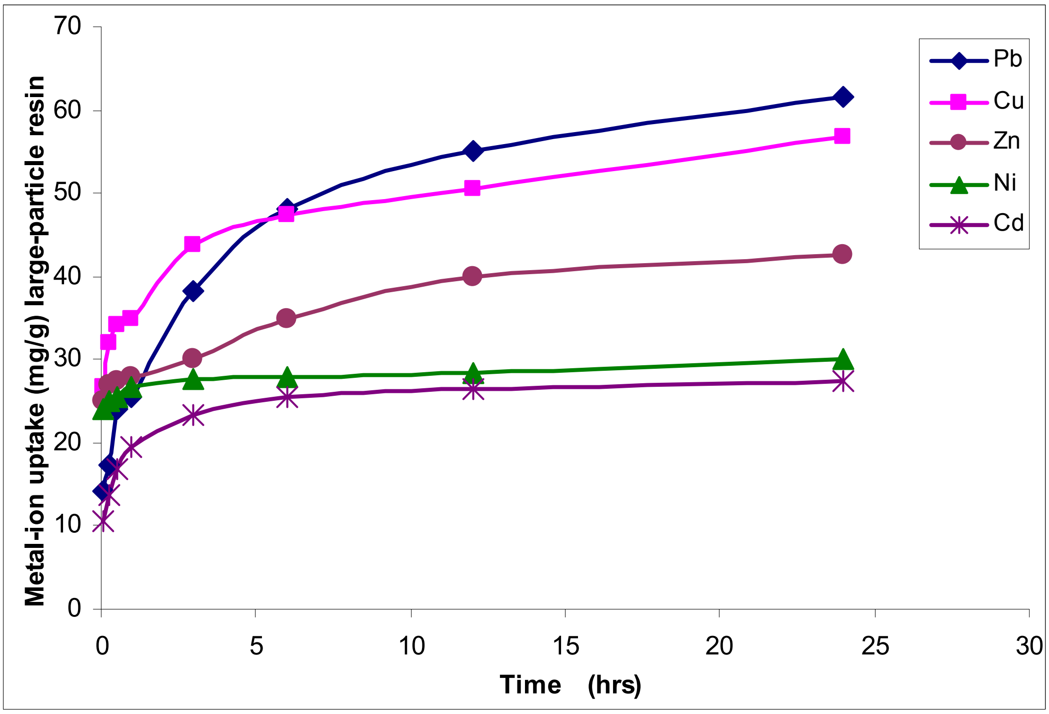


Figure 25. Pb(II), Cu(II), Zn(II), Ni(II), and Cd(II) uptake by resin as a function of contact time.

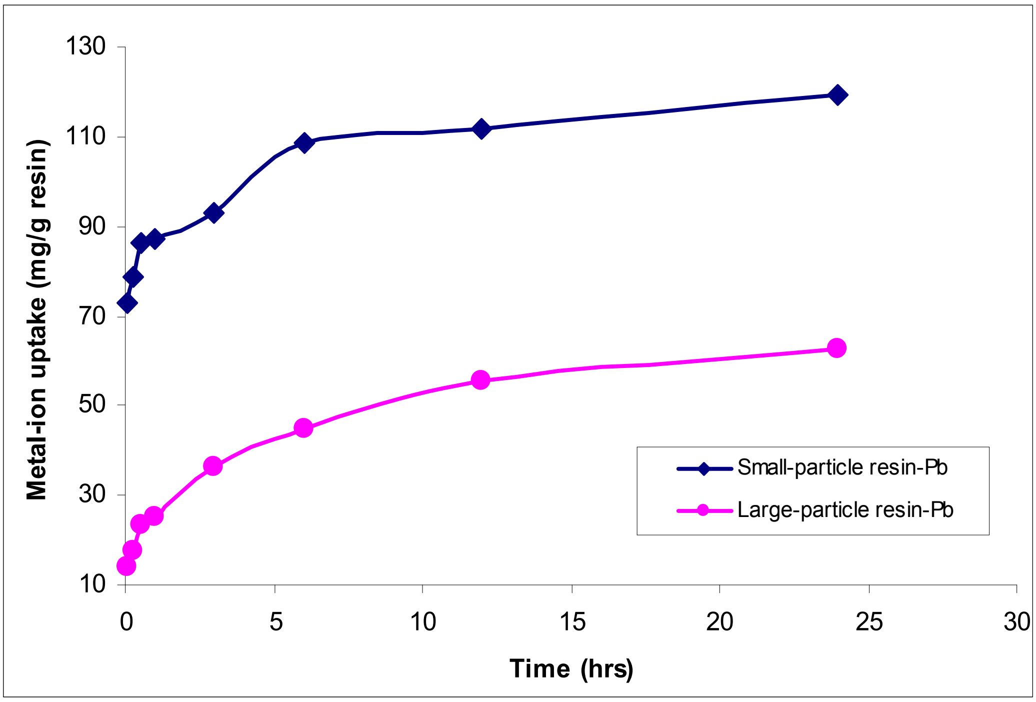


Figure 26. Pb(II) uptake by large and small particle resin as a function of contact time

3.4.2 Effect of pH on metal-ion uptake

The pH dependence of metal ions uptake for chitosan and resin was studied in different acetate buffer solutions in the pH range of 3.0-7.0 under continuous shaking for a fixed contact time of 24 hours at 25 °C. At higher pH values (above 7.0), precipitation of the metal hydroxide takes place which prevented the study of their uptake. The pH-uptake profiles for chitosan are presented in Tables 30 and the results for large-particle resin are presented in Tables 31-35 and Figure 28.

Results reveal that the adsorption of divalent metal ions increases as the pH of the solution increases.

The availability of the hydroxyl oxygen atoms and the lone pairs of electrons on the nitrogen atom on chitosan or sulfur atom on resin are affected by the pH; this may explain the different behaviors at different pH values. First for resin: As pH increases, the hydroxyl group may lose its proton and becomes negatively charged and the sulfur

atoms lone pair will be more available for binding to metal ions and thus, increase the attraction of metallic ions onto the surface. On the other hand, at acidic pH a decrease in the adsorption is attributed to the protonation of complexation sites where a competition between hydrogen and metal ions occurs with an apparent preponderance of hydrogen ions, which restricts the approach of metal cations as a consequence of the repulsive force. This is the same for amine group in chitosan at low pH, protonation of oxygen and nitrogen atoms occurs which makes chitosan soluble in the medium.

Table 30. Lead(II), cupper(II), zinc(II), nickel(II), and cadmium(II) uptake by chitosan as a function of pH. Temperature = 25 ^{o}C, contact time = 6 hour, pH from 6.0 to 7.0, with total ionic strength of 0.10 M. Volume of solution = 50.0 mL containing 25.0 mg of metal and 0.1000 g of the polymer

Metal	pH	Equilibrium Concentration of M(II) in solution (ppm)	Equilibrium Concentration of M(II) adsorbed(ppm)	M(II) uptake (mg/g)	% Uptake
Pb	6.0	475.9	24.02	12.01	4.800
Pb	7.0	472.5	27.44	13.72	5.480
Cu	6.0	267.4	232.6	116.3	46.52
Cu	7.0	258.6	241.4	120.7	48.28
Zn	6.0	398.9	101.1	50.53	20.21
Zn	7.0	392.9	107.1	53.57	21.43
Ni	6.0	415.3	84.70	42.35	16.94
Ni	7.0	411.5	88.50	44.25	17.70
Cd	6.0	281.0	219.0	109.5	43.80
Cd	7.0	271.4	228.6	114.3	45.72

Table 31. Lead(II) uptake by resin as a function of pH. Temperature = 25 ^oC, contact time = 6 hour, pH range from 3.0-7.0, with total ionic strength of 0.10 M. Volume of solution = 50.0 mL containing 25.0 mg Pb(II) and 0.1000 g of the polymer

pH	Equilibrium Concentration of Pb(II) in solution (ppm)	Equilibrium Concentration of Pb(II) adsorbed(ppm)	Pb(II) uptake (mg/g)	% Uptake
3.0	420.8	79.20	35.90	15.84
3.5	415.2	84.80	32.30	16.96
4.0	409.0	91.00	25.40	18.20
5.0	407.6	92.40	29.50	18.48
6.0	391.2	108.8	56.98	21.76
7.0	377.3	122.7	63.35	24.54

Table 32. Cupper(II) uptake by resin as a function of pH. Temperature = 25 ^oC, contact time = 6 hour, pH range from 3.0-7.0, with total ionic strength of 0.10 M. Volume of solution = 50.0 mL containing 25.0 mg Cu(II) and 0.1000 g of the polymer

pH	Equilibrium Concentration of Cu(II) in solution (ppm)	Equilibrium Concentration of Cu(II) adsorbed(ppm)	Cu(II) uptake (mg/g)	% Uptake
3.0	427.3	72.70	22.50	14.54
3.5	422.8	77.20	26.70	15.44
4.0	418.8	81.20	27.50	16.24
5.0	415.8	84.20	29.20	16.84
6.0	403.2	96.80	49.93	19.36
7.0	389.8	110.2	55.21	22.04

Table 33. Zinc(II) uptake by resin as a function of pH. Temperature = 25 ^oC, contact time = 6 hour, pH range from 3.0-7.0, with total ionic strength of 0.10 M. Volume of solution = 50.0 mL containing 25.0 mg Zn(II) and 0.1000 g of the polymer

pH	Equilibrium Concentration of Zn(II) in solution (ppm)	Equilibrium Concentration of Zn(II) adsorbed(ppm)	Zn(II) uptake (mg/g)	% Uptake
3.0	448.5	51.50	25.75	10.30
3.5	443.5	56.50	28.25	11.30
4.0	441.0	59.00	29.50	11.80
5.0	436.8	63.20	31.60	12.64
6.0	428.5	71.50	35.75	14.30
7.0	418.5	81.50	40.75	16.30

Table 34. Nickel(II) uptake by resin as a function of pH. Temperature = 25 ^oC, contact time = 6 hour, pH range from 3.0-7.0, with total ionic strength of 0.10 M. Volume of solution = 50.0 mL containing 25.0 mg Ni(II) and 0.1000 g of the polymer

pH	Equilibrium Concentration of Ni(II) in solution (ppm)	Equilibrium Concentration of Ni(II) adsorbed(ppm)	Ni(II) uptake (mg/g)	% Uptake
3.0	465.6	34.40	17.20	6.88
3.5	461.4	38.60	19.30	7.720
4.0	452.0	48.00	24.00	9.600
5.0	450.6	49.40	24.70	9.880
6.0	445.4	54.60	27.30	10.92
7.0	441.0	59.00	29.50	11.80

Table 35. Cadmium(II) uptake by resin as a function of pH. Temperature = 25 ^{o}C, contact time = 6 hour, pH range from 3.0-7.0, with total ionic strength of 0.10 M. Volume of solution = 50.0 mL containing 25.0 mg Cd(II) and 0.1000 g of the large-particle resin

pH	Equilibrium Concentration of Cd(II) in solution (ppm)	Equilibrium Concentration of Cd(II) adsorbed(ppm)	Cd(II) uptake (mg/g)	% Uptake
3.0	466.9	33.10	16.55	6.62
3.5	460.4	39.60	19.80	7.92
4.0	458.3	41.70	20.85	8.34
5.0	453.6	46.40	23.20	9.28
6.0	450.7	49.30	24.65	9.86
7.0	447.4	52.60	26.30	10.52

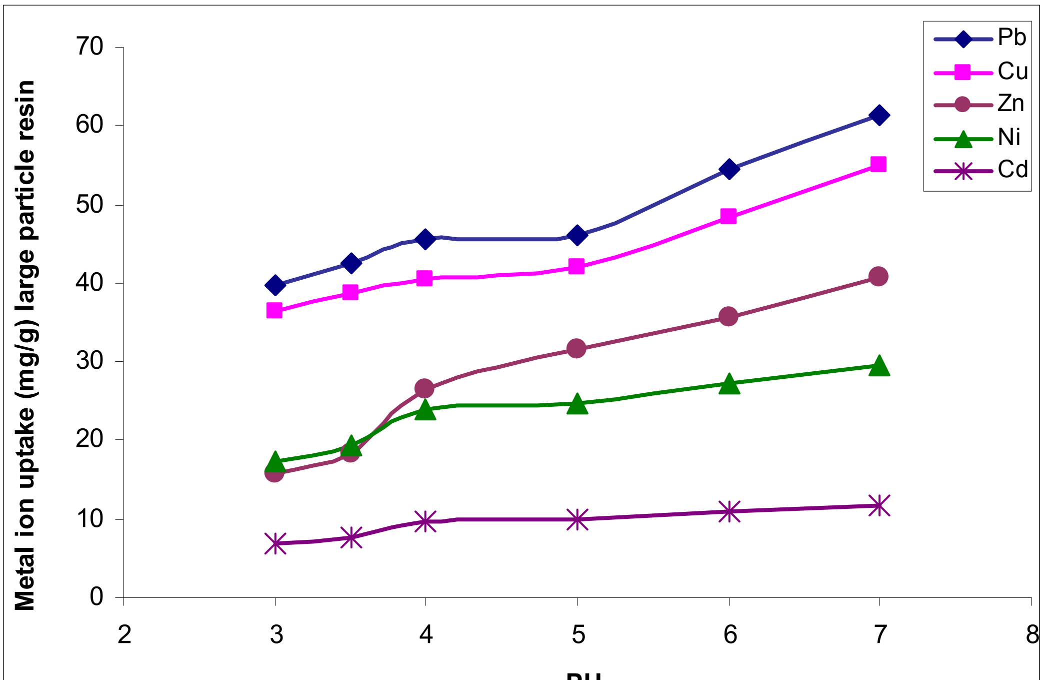


Figure 27. Effect of pH on Pb(II), Cu(II), Zn(II), Ni(II), and Cd(II) uptake by large–particle resin.

3.4.3 Effect of the metal concentration on the metal(II) uptake

The effect of the metal concentration of Pb(II), Cu(II), Zn(II), Ni(II) and Cd(II) on the rate of uptake for resin, was investigated by batch equilibration technique. Suspended 0.1000 g of dry resin samples were equilibrated for 2 hours with 25.0 mL buffer solution of pH = 7.0 with total ionic strength of 0.10 M. An amount of 25.0 mL of different concentrations (275, 300, 350, 400, 450 and 500 ppm) of Pb(II), Cu(II), Zn(II), Ni(II) and Cd(II) solution were added at 25 °C under continuous shaking for 24 hours. Results are presented in Tables 36-40 and Figure 29. The curves show that the metal ion uptake by the resin increases by the increasing the concentration of the metal used. This may be explained by the increase of the metal concentration available for chelation compared to a fixed amount of polymer available in solution.

Table 36. Lead(II) uptake by resin as a function of metal mass. Temperature = 25 °C, contact time = 24 hour, pH = 7.0. Volume of solution = 50.0 mL containing 25.0 mg Pb(II)

Metal concentration (ppm)	Equilibrium Concentration of Pb(II) in solution (ppm)	Concentration of Pb(II) adsorbed (ppm)	Pb(II) uptake (mg/g)	% Uptake
275	6.380	268.6	24.42	97.68
300	77.40	222.6	37.10	74.20
350	195.2	154.8	44.23	44.23
400	269.0	130.9	49.12	32.75
450	320.6	129.4	57.51	28.76
500	373.0	127.0	63.50	25.40

Table 37. Copper(II) uptake by resin as a function of metal mass. Temperature = 25 °C, contact time = 24 hour, pH = 7.0. Volume of solution = 50.0 mL containing 25.0 mg Cu(II)

Metal concentration (ppm)	Equilibrium Concentration of Cu(II) in solution (ppm)	Concentration of Cu(II) adsorbed (ppm)	Cu(II) uptake (mg/g)	% Uptake
275	17.60	257.4	23.40	93.60
300	92.40	207.6	34.60	69.20
350	208.3	141.7	40.50	40.50
400	276.8	123.2	46.20	30.80
450	330.5	119.5	53.10	26.55
500	382.9	117.0	58.52	23.41

Table 38. Zinc(II) uptake by resin as a function of metal mass. Temperature = 25 °C, contact time = 24 hour, pH = 7.0. Volume of solution = 50.0 mL containing 15.0 mg Zn(II)

Metal concentration (ppm)	Equilibrium Concentration of Zn(II) in solution (ppm)	Concentration of Zn(II) adsorbed (ppm)	Zn(II) uptake (mg/g)	% Uptake
275	107.8	167.2	15.20	60.80
300	147.0	153.0	25.50	51.00
350	249.7	100.3	28.65	28.65
400	311.5	88.53	33.20	22.13
450	364.7	85.25	37.89	18.95
500	415.0	85.00	42.50	17.00

Table 39. Nickel(II) uptake by resin as a function of metal mass. Temperature = 25 °C, contact time = 24 hour, pH = 7.0. Volume of solution = 50.0 mL containing 25.0 mg Ni(II)

Metal concentration (ppm)	Equilibrium Concentration of Ni(II) in solution (ppm)	Concentration of Ni(II) adsorbed(ppm)	Ni(II) uptake (mg/g)	% Uptake
275	179.2	95.81	8.710	34.84
300	217.5	82.50	13.75	27.50
350	287.5	62.48	17.85	17.85
400	347.5	52.53	19.70	13.13
450	400.5	49.50	22.00	11.00
500	441.2	58.80	29.40	11.76

Table 40. Cadmium(II) uptake by resin as a function of metal mass. Temperature = 25 °C, contact time = 24 hour, pH = 7.0. Volume of solution = 50.0 mL containing 25.0 mg Cd(II)

Metal concentration (ppm)	Equilibrium Concentration of Cd(II) in solution (ppm)	Concentration of Cd(II) adsorbed(ppm)	Cd(II) uptake (mg/g)	% Uptake
275	204.1	70.95	6.450	25.80
300	241.7	58.32	9.720	19.44
350	311.4	38.64	11.04	11.04
400	364.9	35.15	13.18	8.79
450	409.2	40.79	18.13	9.07
500	448.4	51.60	25.80	10.32

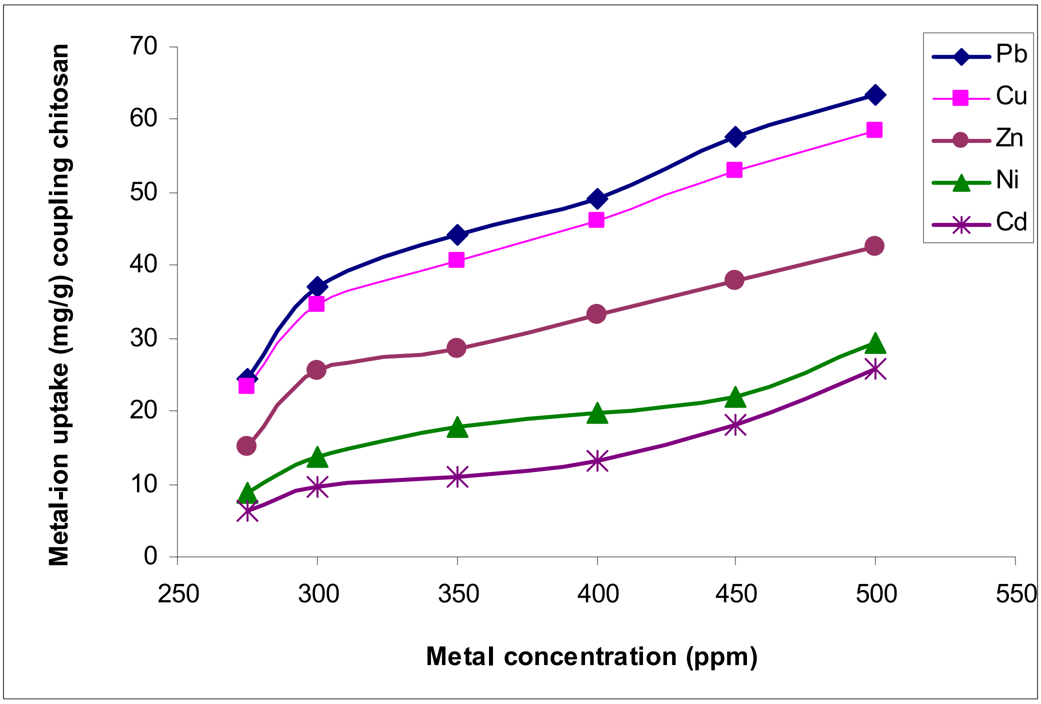


Figure 28. Pb(II), Cu(II), Zn(II), Ni(II), and Cd(II) uptake by resin as a function of metal ion concentration.

3.4.4 Effect of the polymer mass on the metal(II) uptake

The effect of the polymer mass on the rate of lead(II) uptake for large and small particle resin was investigated by a batch equilibration technique. Suspensions of different ,masses of (0.1000, 0.2000, 0.4000, 0.6000 and 0.8000 g) of large and small particle resin samples were equilibrated for 2 hours with 25.0 mL buffer solution of pH = 7.0 with total ionic strength of 0.20 M. An amount of 25.0 mL of 500 ppm of Pb(II) solution was added at 25 °C under continuous shaking for 24 hours. The results are presented in Tables 41-42 and Figure 30. Results reveal that the percentage of Pb(II) adsorption by the large and small particle resin increases by the increase of the mass of the polymer used and small-particle resin displays higher metal-ion uptake than large-particle resin. This may be explained by the increase of the polymers sites available for

chelation compared to a fixed amount of Pb(II) ions available in solution and small-particle resin due to their high surface areas and filtration capacity**.**

Table 41. Lead(II) uptake by large resin as a function of polymer mass. Temperature = 25 °C, contact time = 6 hour, pH = 7.0. Volume of solution = 50.0 mL containing 25.0 mg Pb(II)

Polymer mass (g)	Equilibrium Concentration of Pb(II) in solution (ppm)	Concentration of Pb(II) adsorbed(ppm)	Pb(II) uptake (mg/g)	% Uptake
0.10	403.6	96.40	48.20	19.28
0.20	355.8	144.2	36.05	28.84
0.40	343.6	156.4	19.55	31.28
0.60	285.3	214.7	17.89	42.94
0.80	230.2	269.8	16.86	53.96

Table 42. Lead(II) uptake by small resin as a function of polymer mass. Temperature = 25 °C, contact time = 6 hour, pH = 7.0. Volume of solution = 50.0 mL containing 25.0 mg Pb(II)

Polymer mass (g)	Equilibrium Concentration of Pb(II) in solution (ppm)	Concentration of Pb(II) adsorbed(ppm)	Pb(II) uptake (mg/g)	% Uptake
0.10	350.4	149.6	74.82	29.93
0.20	308.30	191.7	47.93	38.34
0.40	206.8	293.2	36.65	58.64
0.60	122.9	377.1	31.43	75.42
0.80	100.1	399.9	24.99	79.98

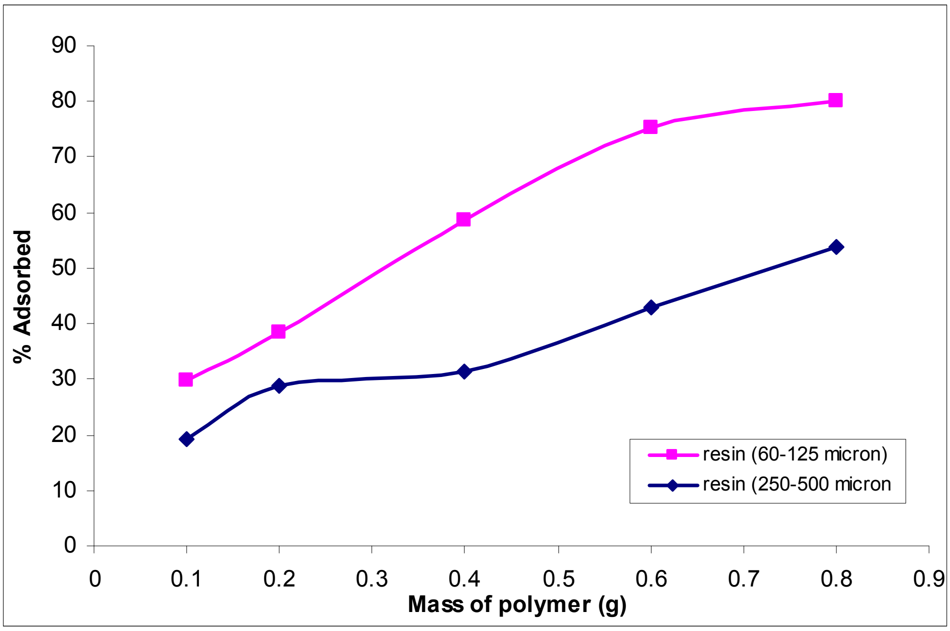


Figure 29. Effect of the polymer mass on % of Pb(II) adsorbed by small and large particle resin

3.4.5 Adsorption kinetics

The effect of contact time and the initial Pb(II) ions concentration on the adsorption rate, equilibrium concentration and equilibrium loading capacity of Pb(II) ions on large and small particle resin are shown in Figures 19-22. Results reveal that the amount of Pb^{2+} adsorbed, Q_t, increases with time for all initial concentrations. However, the time needed to reach equilibrium is the same for large and small particle resins. In addition, the uptake rate of the Pb^{2+} ions decreases with time until it approaches a pseudo steady state value known as the equilibrium loading capacity, Q_e. The contact time needed to reach equilibrium conditions was about 12 h in the case of large and small particle resins.

The loading capacity in the first hour, Q_4, for large and small particle resins were 45.4 and 87.09 mg/g, respectively. However, the loading capacity at 12 hours, Q_7 for large and small resin were 55.00 and 111.8 mg/g, and Q_8 for the large and small particle resin were 63.50 and 119.2 mg/g for large and small particle resin, respectively. These results

indicate that the mechanism of adsorption in large and small particle resin are similar and pore diffusion (intraparticle diffusion could play an important role in the adsorption process).

As previously mentioned, four kinetic models can be used to examine the mechanism of the adsorption process; pseudo first order, pseudo second order, Elovich, and intraparticle diffusion models; fitting results of the experimental data are shown in Figures. 31, 32, 33, and 34 for the four models, respectively.

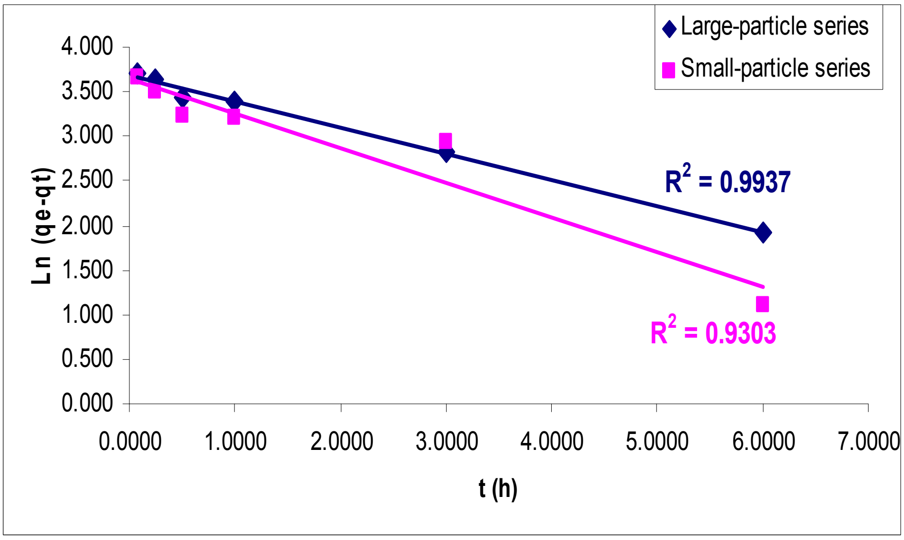


Figure 30. Pseudo-first-order kinetics for adsorption of Pb(II) ions onto resin for large and small particle resin at 25 °C.

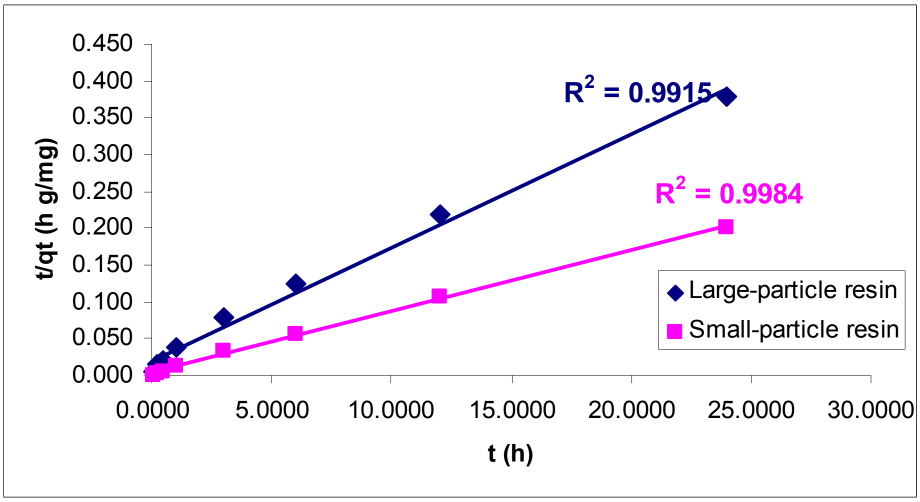


Figure 31. Pseudo-second-order kinetics for adsorption of Pb(II) ions onto resin for large and small particle resin at 25 °C.

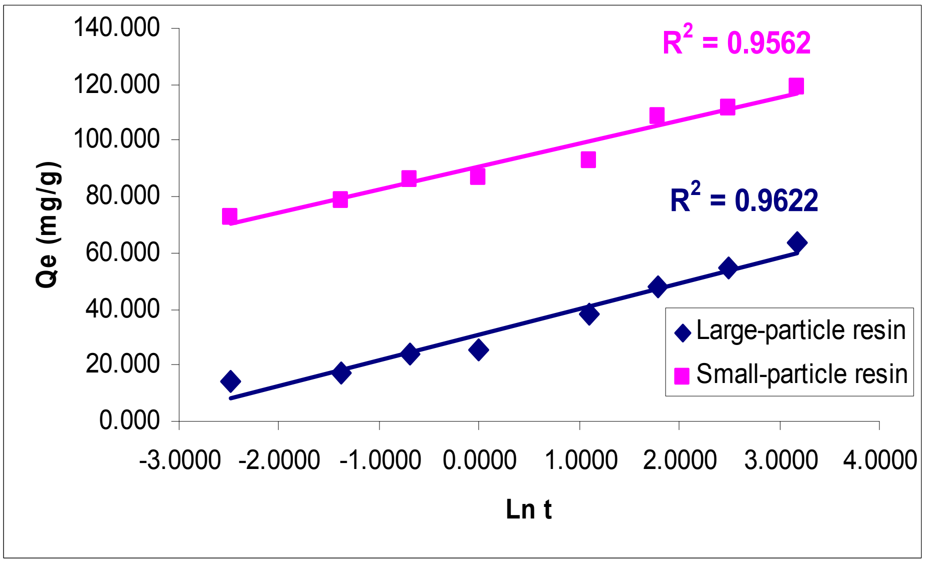


Figure 32. Elovich model for adsorption of Pb(II) ions onto resin for large and small particle resin at 25 °C.

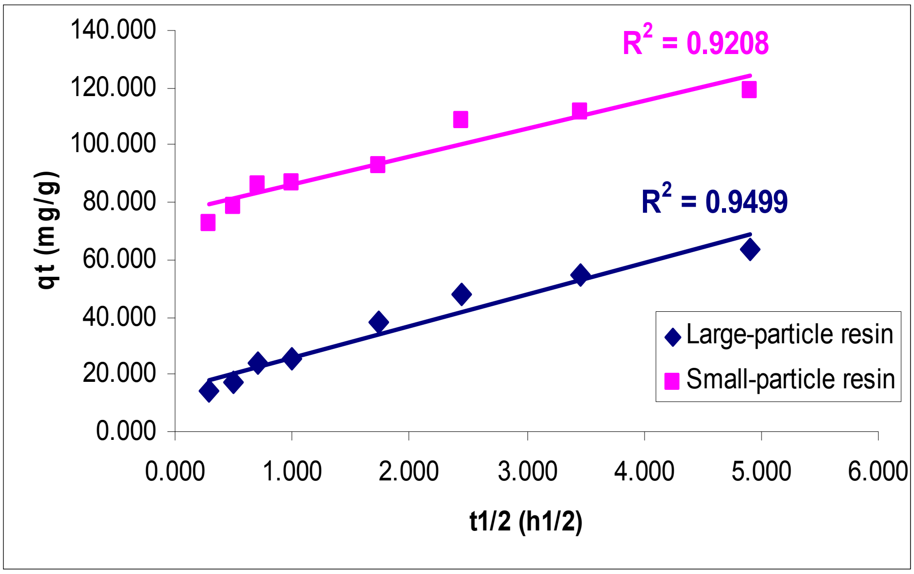


Figure 33. Intraparticle diffusion model for adsorption of Pb(II) ions onto resin for large and small particle resin at 25 °C.

In addition to experimental and predicted values of $Q_{e,}$ the constants for the four models, ,are given in Table 43. Results from the Figures show that the Pb(II) ion adsorption by the resin is best described by the pseudo-second order model and by Elovich model. This is confirmed by the values of R^2 shown in Table 43, which are close to unity for the pseudo second order and the Elovich models, and less than 0.99, and 0.94 for the pseudo first order and intraparticle diffusion models, respectively. In addition, the values of predicted Q_e in the case of the second order model are very close to the experimental values for all Pb(II) ions initial concentrations. For example, when the initial concentration of Pb(II) ions was 500 mg/L and the temperature was 25°C, the experimental $Q_{e,}$(exp) for large and small particle resins after 12 h were 55.00 and 111.8 mg/g, respectively. On the other hand, the predicted values for the large and small particle resin, Q_e,(calc) by the pseudo second order were 64.96 and 119.5 mg/g, respectively. The validity of the four models was further verified using the sum of squared errors, SSE, %; the values of SSE, % are given in Table 43.

Table 43. Comparison of the pseudo-first-order, pseudo-second-order, Elovich and intraparticle diffusion models for large and small particle resins at Pb(II) ions initial concentration of 500 ppm at 25 °C.

Pseudo-first-order kinetic model					
Resin	**$Q_{e,exp}$ (mg/g)**	**$Q_{e,calc.}$ (mg/g)**	**K_1 (h^{-1})**	**R^2**	**SSE (%)**
Large particle	55.00	39.57	0.674	0.994	5.657
Small particle	111.8	38.21	0.893	0.930	26.02
Pseudo-second-order kinetic model					
Large particle	55.00	64.96	0.012	0.992	3.525
Small particle	111.8	119.51	0.022	0.998	2.727
Elovich kinetic model					
Resin	**$Q_{e,calc.}$ (mg/g)**	**α mg g^{-1} min^{-1}**	**B mg g^{-1} min^{-1}**	**R^2**	**SSE (%)**
Large particle	60.19	280.92	0.110	0.962	1.834
Small particle	116.9	47.61×10^4	0.121	0.956	1.800
Intraparticle diffusion model					
Resin	**$Q_{e,calc.}$ (mg/g)**	**K_p**	**X_i**	**R^2**	**SSE (%)**
Large particle	68.86	10.98	15.09	0.949	4.900
Small particle	119.5	8.344	78.59	0.921	2.710

As presented in Table 43, the SSE % values are relatively low for the pseudo second order and Elovich models compared to those of the pseudo first order and intraparticle diffusion models. These results indicate that the adsorption of Pb(II) ions on the resin is best described by the pseudo-second order model and that the pseudo-first-order and intraparticle diffusion models were not suitable for the interpretation of the adsorption mechanism within the concentration range under study, this is in agreement with the results obtained by other researchers.

3.4.6 Adsorption thermodynamics

Results presented earlier showed that the adsorption capacities of the large and small particle resins increase as the temperature increases. For example, Q_{max} for small particle resin increases from 109.7 to 122.6 mg/g as the temperature increases from 25 °C to 35 °C. This result confirms the endothermic nature of the adsorption of Pb^{2+} onto chitosan polymers. The increase in the adsorption capacity with temperature may suggest that the active surface centers available for adsorption have increased with temperature. This increase could be explained as follows: As the temperature increases the pore size could increase and the liquid phase viscosity decreases; this will enhance the rate of intraparticle diffusion of solute.

Calculation of the thermodynamic parameters for the adsorption process was accomplished by using equations 14 and 15. The variation of the distribution coefficient, K_d, with temperature for the large and small particle resin at three Pb^{2+} initial concentrations of 50, 100 and 150 mg/L are presented in Tables 44-45 and Figures 35, 36 and 37.

Table 44. Variation of distribution coefficient (K_d) as function of a temperature for large size resin at pH = 7, contact time = 12 hours, total ionic strength of 0.10 M, and total volume of solution = 50.0 mL containing 50 mg/L Pb(II) and 0.1000 g polymer

Resin size	T (K)	C_e (ppm)	C_{Ae} (ppm)	K_d
C_o= 50 mg/L				
Large	288.15	23.70	26.30	1.110
	298.15	17.00	33.00	1.941
	308.15	13.30	36.70	2.759
Small	288.15	10.30	39.70	3.854
	298.15	5.300	44.70	8.434
	308.15	1.400	48.60	34.71
C_o= 100 mg/L				
Large	288.15	50.80	49.20	0.969
	298.15	39.60	60.40	1.525
	308.15	32.20	67.80	2.106
Small	288.15	21.20	78.80	3.717
	298.15	12.50	87.50	7.000
	308.15	7.800	92.20	11.82
C_o= 150 mg/L				
Large	288.15	81.40	68.60	0.843
	298.15	69.00	81.00	1.174
	308.15	57.20	92.80	1.622
Small	288.15	50.90	99.10	1.947
	298.15	30.60	119.4	3.902
	308.15	22.40	127.6	5.696

Table 45. The thermodynamic functions concerning of the adsorption process of Pb(II) onto resin at different temperature values.

	Δ G° (J/mol)			Δ H° kJ/mol	Δ S° J/ K mol
resin	**T = 15 °C**	**T = 25 °C**	**T = 35 °C**		
C_o= 50 mg/L					
Large	-249.376	-1644	-2600	33.73	118.1
Small	-3232.268	-5285	-9087	80.95	291.5
C_o= 100 mg/L					
Large	76.668	-1046	-1907	28.74	99.59
Small	-3145.315	-4677	-6327	42.78	159.5
C_o= 150 mg/L					
Large	409.8	-397.5	-1239	24.19	82.52
Small	-1596	-3374	-4457	39.78	143.9

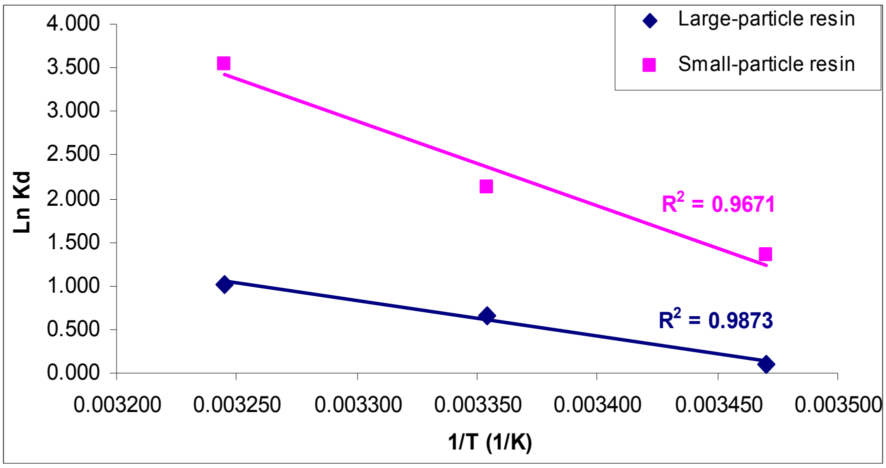


Figure 34. Log K_d of Pb(II) as a function of temperature for 50 mg/L of resin.

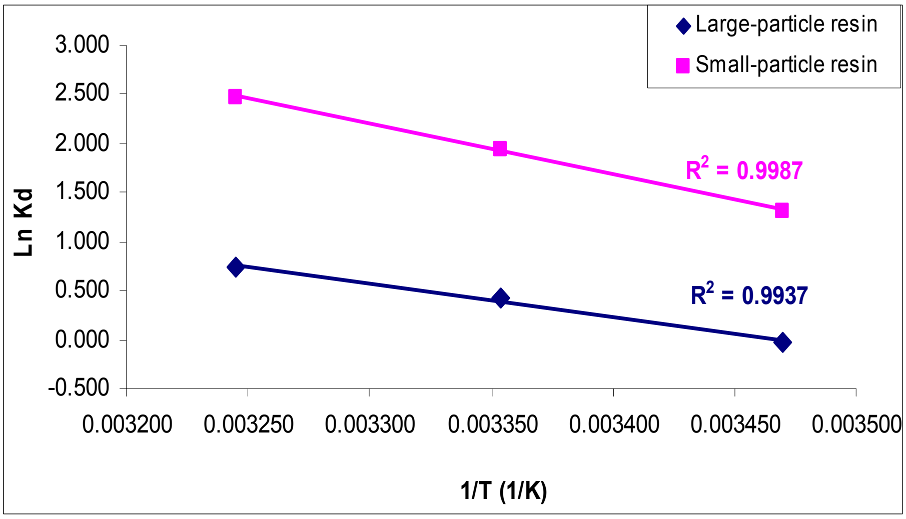


Figure 35. Log K_d of Pb(II) as a function of temperature for 100 mg/L of resin.

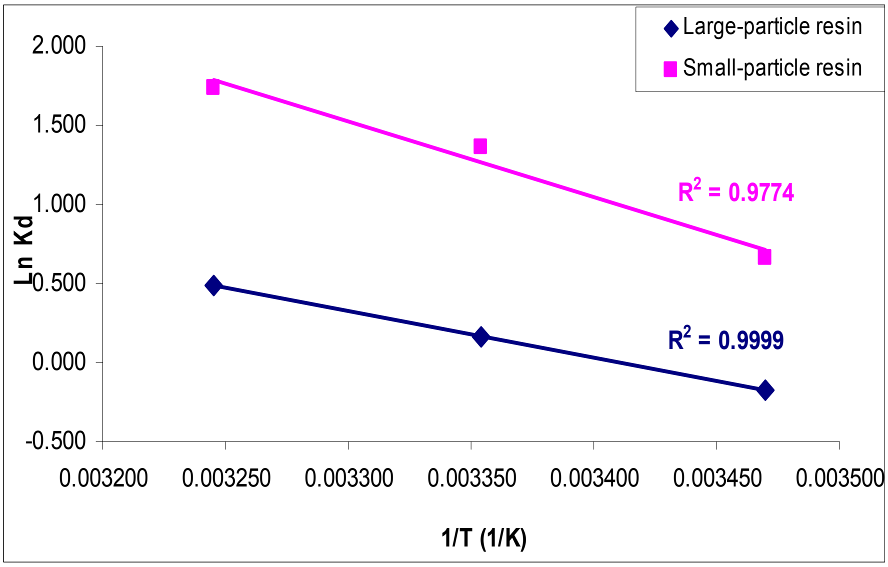


Figure 36. Log K_d of Pb(II) as a function of temperature for 150 mg/Lof resin

As shown in Table 3.43, K_d values increase for small and large particle resins as the temperature increases. This confirms the endothermic nature of the adsorption process. However, the values of K_d at 150 mg/L are lower than those at 100 and 50 mg/L. This indicates the feasibility of the adsorption process if Pb(II) ions initial concentration is

not high enough. The standard enthalpy ΔH^o and at two different concentrations was calculated from the relationship between $\ln k_d$ and 1/T; it is linear with high correlation coefficient R^2 in was about 0.960 only. Table 3.44 lists values of the thermodynamic parameters of the adsorption process for Pb(II) ions at three initial concentrations, 50, 100 and 150 mg/L. when C_o = 50 mg/L, the standard free energies, ΔG^o for large and small particle resin are negative and decrease from -249.4 to -2600 J/mol and from -3232 to -9087 J/mol as the temperature increases from 15 ^oC to 35 ^oC, respectively. These results indicate the spontaneous nature and feasibility of the process in the case of polymer when the initial concentration of Pb(II) ions is 50 g/L. On the other hand, if the initial concentration increases to 100 and 150 mg/L, ΔG^o is still negative for small particle resin while positive for large particle resin at 15 ^oC and starts to decrease as the temperature increases.

In addition, the table shows positive values of ΔH^o and the standard entropy ΔS^o for large and small particle resin at the three initial concentrations. This was previously confirmed by the isotherm experiments at different temperatures. The positive values of standard entropy, ΔS^o indicates the affinity of the resin for adsorbates such as Pb(II) ions as a result of the increased randomness at the interface between the solid liquid phases although the values of ΔS^o were found to decrease as the initial concentration increases. These results could represent a strategy for heavy metals adsorption such as Pb(II) on polymeric materials. Best results could be obtained when the ion concentration is relatively low and the temperature is relatively high.

3.4.7 Column Experiments

3.4.7.1. Metal ion uptake by resin

The metal ion uptake by resin using column technique was determined for Pb(II), Cu(II), and Zn(II) ions at pH 7.0 and 25 °C. The initial concentration for each metal ion was 1000 ppm and flow rate was 1.0 mL/min. The results are expressed as percent metal ion uptake by the column and are presented in Table 46.

Table 46. The percent of metal ion uptake by resin using column experiment

Metal Ion	Initial Conc. (ppm)	Final Conc. (ppm)	Loaded Conc. (ppm)	% Uptake
Pb(II)	1000	113.6	886.4	88.64
Cu(II)	1000	212.1	787.9	78.79
Zn(II)	1000	305.8	694.2	69.42

It is observed that the % of uptake in column experiment is less than that obtained in batch experiments, probably because it takes longer time to achieve complete saturation. On the other hand, the shaking process in batch technique is a fundamental factor which may increase the % uptake of metal ions compared to column technique and the adsorption of lead ions was the highest because the resin high selective to the lead.

3.4.7.2 Desorption studies

The main aim of this study is to determine the capability of resin to be regenerated for further uses. A volume of 50 mL of each of 1 M HNO_3, 0.5 H_2SO_4 and 0.1 M EDTA were used for elution of sorbent (adsorbed metal ion) at a flow rate of 1 mL/min. The metal ion in eluent was collected in five 10-mL portions, and the concentrations were

determined using atomic absorption spectrometry (AAS). The results are presented in Tables 47, 48 and 49.

Table 47. Desorption of Pb(II) and the regeneration process

Pb(II) ion on resin	HNO_3	H_2SO_4	EDTA
% Recovery (First washing)	33.55	3.920	18.09
% Recovery (Second washing)	18.86	1.910	9.300
% Recovery (Third washing	12.89	1.590	6.840
% cumulative Recovery	65.30	7.420	34.23

Table 48. Desorption of Cu(II) and the regeneration process

Cu(II) ion on resin	HNO_3	H_2SO_4	EDTA
% Recovery (First washing)	15.17	16.30	14.42
% Recovery (Second washing)	4.610	11.06	11.06
% Recovery (Third washing	4.490	8.200	8.400
% cumulative Recovery	24.27	35.56	33.88

Table 49. Desorption of Zn(II) and the regeneration process

Zn(II) ion on resin	HNO_3	H_2SO_4	EDTA
% Recovery (First washing)	26.42	30.46	22.80
% Recovery (Second washing)	5.450	7.700	6.070
% Recovery (Third washing	4.520	6.910	4.490
% cumulative Recovery	36.39	45.07	33.36

From these tables, it is clear that HNO_3 solution was most effective desorbing agent among the three reagents, and that its effectiveness was in the order: Pb(II)>Zn(II)>Cu(II), while for H_2SO_4 the order was Zn(II)>Cu(II)>Pb(II, and for EDTA the order was Pb(II)>Zn(II)>Cu(II). These results reflect the capability of the resin to coordinate to the metal ions compared to EDTA, and that the 1-hydroxy-2-pyridinethione group can form stable complexes at low pH.

3.5 Conclusion

The present work has focused on the preparation, characterization, and isothermal properties of a new resin obtained from chitosan and 1-hydroxy-2-pyridinethione-4-carboxylic acid. The resin was characterized by IR spectroscopy, elemental analysis, and thermal techniques. The chelation properties of the resin toward some divalent metal ions have been investigated by batch equilibration method under different experimental conditions of contact time, pH, mass of resin, particle size, amount of metal ion, and temperature.

❖ Results indicate that the adsorption of Pb(II) ions by the resin is a favourable process where the uptake increases as temperature, contact time, PH, metal concentration and polymer mass increase and size of resin decrease.

❖ Both Langmuir and Freundlich adsorption models were well applicable for Pb(II) adsorption by the resin. Langmuir adsorption models best fits the experimental data since it presents the greater correlation coefficients for all temperatures with values more than 0.99 for large-particle resin and 0.98 for small particle resin which indicates a homogeneous sorption of lead(II) ions on the polymers surfaces.

- ❖ The adsorption of Pb(II) ions on the resin is best described by the pseudo-second order and elovich model.
- ❖ pH binding capacity profiles showed that divalent metal ion uptake of the resin increases with increasing pH, and approaches the highest uptake value at pH 7.
- ❖ The percent of uptake in column experiment is less than obtained in batch experiments.
- ❖ The result of the standard free energy, standard enthalpy and standard entropy indicate the spontaneous and feasibility of the process.
- ❖ Nitric acid was most effective desorbing agent.

REFERENCES

Abu-Dari, K. (1979), Thiohydroxamate and Hydroxamate Transtion Metal Complexes, **Dissertation**, University of California, Berkeley.

Abu-Dari, K. (1988). Synthesis and characterization of lead and cadmium thiohydroxamate complexes. **Dirasat**, 15(9), 96-101.

Abu- Dari, K., Hahn, F., and Raymond, K., (1990). "Lead sequestering agent 1. synthesis, physical properties and structure of Thiohydroxaniato Complexes". **J. Am. Chem. Soc.,** 112, 1519-1524.

Abu-Dari, K. and Raymond, K. N. (1991), Ferric Ion Sequestring Agents. Synthesis of Tris(hydroxypyridinethione) Ligands and Their Ferric Complexes; X-ray Structure Analysis of N,N', N''-Tris((1,2dideydro-1-hydroxy-2-thioxopyrid-6-yl)carbonyl)-2,2,2-triamino-triethylaminato)iron(III), **Inorg.Chem.**, 30, 519-524.

Abu-Dari, K. Karpishin, T. B. and Raymond, K. N. (1993), Lead Squestring Agents. 2. Synthesis of Mono- and Bis(hydroxypyridinethione) ligands and Their lead Complexes. Structure of Bis(6-(diethylcarbonyl)-1-hydroxy-2(1H)-pyridine-2-thionato-O, S)lead(II), **Inorg. Chem**., 32, 3052-3055.

Al-Khabbas, M., (2007). " 1-Hydroxy-2-pyridinethiones; synthesis, lead and zinc complexes and study their efficacy in treatment of lead poisoning". University of Jordan, Amman -Jordan

Al-Thawabeyeh, R., (2004), Synthesis, characterization and stability constants of lead and cadmium complexes of amine and amino acid derivative of 1-hydroxy-2-pyridinethione-4-carboxylic acid, University of Jordan, Amman –Jordan.

Anne, E. V. G. Xu, . and Raymond, K. N. (2003), Rational Design Of Squestering Agents for Plutonium and Other Actinides, **Chem. Rev**., 103, 4207-4282.

An, X. Su, Z. Zeng, H. (2003), Preparation of highly magnetic chitosan particles and their use for affinity purification of enzymes, J. Chem. Technol. Biotechnol. 78, 596-600.

Ata, S. (2009), Investigation of Reversing Adverse Biochemical Effect of Lead Poising BY N,N`-BIS[(1,2-Didehydro-1-Hydroxy-2-Thiopyrid-4-yl)-Carbonyl]-L-Lysine. **Dissertation**, chemistry, Jordan University.

Atkins, P.; Overton, T.; Rourke, J.; Weller, M.; Spiro, T.; Stiefel, E. (2006*),* Shriver and Atkins Inorganic Chemistry Fourth Edition, W. H. Freeman and Company, New York, 220–224, 460–472.

Atia, A. A. Donia, A. M. Yousif, A. M. (2003), Synthesis of amine and thio chelating resins and study of their interaction with zinc(II), cadmium(II) and mercury(II), React. **Funct. Polym**., 56, 75–82.

Bell, C.; Smith, S.; Whittaker, M.; Whittaker, A.; Gahan, L.; Monteiro, M. (2006), Surface-functionalized polymer nanoparticles for selective sequestering of heavy metals, **Advanced Materials**, 18, 582–586.
Bond, A. and Jones, W. (1999), 1-Hydroxy-2(1H)-pyridinethione, **Acta. Cryst**., C55, 1535-1538.

Buckley, J. A. (1985). Preparation of Chelex-100 resin for batch treatment of sewage and river water of ambient pH and alkalinity. **Anal. Chem**., 57, 1488-1490.

Casellato, U. Vigato, P. A. and Tamburini, S. (1983), Thorium Complexes with Bidendate Ligands. Crystal Structure of Dimethylformaidetetrakis(1-oxo-2-thiopyridinato) Thorium(IV), **Inorg. Chim. Acta, 95, 37-42.**

Chanthateyanonth, R. Ruchirawat, S. Srisitthiratkul, C. (2010), Preparation of New Water-Soluble Chitosan Containing Hyperbranched-Vinylsulfonic Acid Sodium Salt and Their Antimicrobial Activities and Chelation with Metals, **Journal of Applied Polymer Science,** DOI 10.1002/app.

Cheung, J.C.Y. Ng, W.H. McKay, G. (2003), Equilibrium studies for the sorption of lead from effluents using chitosan, **Chemosphere**, 52, 1021–1030.

Chiou, T. (2002), **Partition and Adsorption of Organic Contaminants in Environmental systems**, John Wiley and sons, Canda, INC., Publication.

Collier, J. Camp, T. (2000), Synthesis and characterization of polypyrrole/hyaluronic acid composite biomaterials for tissue engineering, **Journal of Biomedical Materials Research Part A**, 50: 574-584.

Covelo, E. Vega, F. and Andrade, M. (2007), Heavy Metal Sorption and Desorption Capacity of Soils Containing Endogenous Contaminants, **Journal of Hazardous Materials**, 143, 419-430.

Cunliffe, D. Pennadam, S. and Alexander, C. (2003), Synthetic and biological polymers—merging the interface,**European Polymer Journal,** 40, 5–25.

Donia, A.M. Atia, A. A. El-Boraey, H. A. Mabrouk, D. (2006), Uptake studies of copper(II) on glycidyl methacrylate chelating resin containing Fe2O3 particles, Sep. **Purif. Technol**. 49, 64–70.

Donia, A.M. Atia, A. A. El-Boraey, H. A. Mabrouk, D. (2008), Adsorption of Ag(I) on glycidyl methacrylate/N,N-methylene bis-acrylamide chelating resins with embedded iron oxide, Sep. **Purif. Technol**. 48, 281-287

Donohue, J. (1956). The structure of oxime. **J.Am.Chem.Soci**., 78,4172-4174.

Ebraheem, K.A.K., Mubarak, M.S., Yassien, Z.J., and Khalili, F. (2000). Chelation properties of poly (8-hydroxyquinoline 5,7-diylmethylene) crosslinked with bisphenol-A toward lanthanum(III), Cerium(III), Neodimium(III), Samarium(III), and Gadolinum(III) ions. **Separation Science and Technology**, 35 (13), 2115-2125.

Ebraheem, K. Mubarak, M. S. Gharabli, (2001) **J. Saudi Chem. Soc**.; Vol.5, No. 3; 399.

Eugene, K.(2001), **Chitin: Fulfilling a Biomaterials Promise** , first edition, Elsevier Science.

Eric. G. (2003), Interactions of metal ions with chitosan-based sorbents, **Separation and Purification Technology,** 38, 43–74.

Fuqiang, L., Jinlong, C., Aimin, L., Zhenghao, F., Junjie, G. and Quanxing, Z. (2004), Equilibrium adsorption of single component and binary mixtures of aromatic compounds onto a polyfunctional Hypercrosslinked polymeric Adsorbent. **Adsorp. Sci. and Tech.**, 22, 13-24.

Gerente, C. Lee, V. K. C. LE Cloirec, P.and Mckay, V. (2007), Application of Chitosan for the Removal of Metals From Wastewaters by Adsorption-Mechanisms and Models, **Critical Reviews in Environmental Science and Technology**, 37:41–127, 2007.

Gordon, M. and Porter, F. J. (1997), Equilibrium Parameters for the Sorption of Copper, Cadmium and Zinc Ions onto Peat 1 Department of Chemical Engineering, The Hong Kong University of Science and Technology, Clear Water Bay, Kowloon, Hong Kong , **Chem. T ech. Biotechnol**, 69, 309-320

Gotoh, T. Matsushima, K.. Kikuchi, K.I. (2004), Adsorption of Cu and Mn on covalently cross-linked alginate gel beads, **Chemosphere**, 55, 57–64.

Gregor, H., and Taifer, M. (1952). Chelate ion exchange resins. **Indust. Eng. Chem**., 44, 2834-2839.

Hall, L. D., & Yalpani, M. (1980). Enhancement of the metal-chelating properties of chitin and chitosan. **Carbohydrate Research**, 83, C5–C7.

Henryk, M. Dorota, B. Maria Najder, W. K. (2002), Synthesis and induction of apoptosis in B cell chronic leukemia by diosgenyl 2-amino-2-deoxy-β-D-glucopyranoside hydrochloride and its derivatives, **Carbohydrate Research**, 338,133–141

Hubert, M. (1971). Antibiotics and other naturally occurring hydroxamic acids and hydroxamates. **Pure.Appl.Chem**., 28 (4), 603-636.

Igwe, J. Abia, A.(2007), Adsorption isotherm studies of Cd, Pb, and Zn (II) ions bioremediation from aqueous solution using unmodified and EDTA-modified maiz cob, **Ecletica Quimica,** 32-33.

Ho, Y. S. and McKay, G. (1998), Sorption of dye from aqueous solution by peat, **Chem. Eng. J.,** 70-115.

Jiang, X., and Whitesides, G. M. (2003), Engineering microtools in polymers to study cell biology, **Eng. Life Sci**., 3,475-480.

Jose´ E. dos Santosa, 1, E. Dockala, R, Cavalheirob, E´ der T.G. (2005), Synthesis and characterization of Schiff bases from chitosan and salicylaldehyde derivatives, **Carbohydrate Polymers**, 60, 277-282.

Langmuir, (1918), the adsorption of gases on plane surfaces of glass, mica and platinum, **J. Am. Chem. Soc.** 40, 1362-1403.

Lebrun, L.; Vallée, F.; Alexandre, B.; Nguyen, Q. (2007), Preparation of Chelating Membranes to removal metal cations from aqueos solution , **Letters,** 207, 9-23.

Li, C.; Cheng, C.; Choo, K.; Yen, W. (2008), Polyelectrolyte enhanced ultrafiltration (PEUF) for the removal of Cd(II): effects of organic lignads and solution pH, **Chemosphere**, *72*, 630-635.

Limin. Z. Jianping, B Xua, X. and Lianga, Z. L. (2010), Adsorption of platinum(IV) and palladium(II) from aqueous solution by magnetic cross-linking chitosan nanoparticles modified with ethylenediamine, **Journal of Hazardous Materials**, 182, 518–524

Low, M. J. D. (1960), Kinetics of chemisorption of gases on solids, **Chem. Rev**. 60-267.

Kavitha, D. Namasivayam, C. (2007). Equilibrium, kinetics and thermodynamics study on biosorption of Cr(VI) by fresh biomass of Saccbaromyces cerevisiae , **Technol.** 98-14.

Kantipuly, C., Katragadda, S., Chow, A., and Gesser, H.D. (1990). Chelating polymers and related supports for separation and preconcentration of trace metals. **Talanta**, 37 (5), 491-517.

Kocaoba, S. Akyuz, T. (2005), Effects of conditioning of sepiolite prior to cobalt and nickel removal, **Desalination**, 181, 313–318.

Krishnapriya, K. R. Kandaswamy, M. (2010), A new chitosan biopolymer derivative as metal-complexing agent: synthesis, characterization, and metal(II) ion adsorption studies, Department of Inorganic Chemistry, University of Madras, Chennai 600 025, India a r t, **Carbohydrate Research**, 345, 2022.

MaKay, G. and Porter, J. F. (1997). Equilibrium parameters for the sorbtion of copper, cadmium and zinc ions onto peat. **J. Chem. Tech. Biotechnol**., 69, 309-320

Masboun, T. and Julian, D. (2004), Characterization of interactions between chitosan and anionic surfactant, Journal of agriculture and food chemistry, (4), 987-91.

McClements, J. (2004), Influence of pH, Ionic Strength, and Temperature onSelf-Association and Interactions of Sodium Dodecyl Sulfate in the Absence and Presence of Chitosan**, Langmuir**, 21, 79-86

Meng,W. W. Chuan, K. Buenda, D. Rogel, B. Maria, L. P. and Dalida, B (2010), Adsorption of copper (II) and lead (II) ions from aqueous solution on chitosan-coated sand, **Carbohydrate Polymers**, 80, 891-899.

Micioi, M. Albu, A. Mateescu, C. Voicu, G. Rusen, E. Marculescu, B. and Mutihac, L. (2007), New polymeric structures designed for the removal of Cu(II) ions of aqueos solutions, **J. Applied Polymer Science**, 103, 1397-1405.

Monier, M., Ayadb, D.M. and Weia, Y. Sarhanb, A.A. (2010),Adsorption of Cu(II), Co(II), and Ni(II) ions by modified magnetic chitosan chelating resin, **Journal of Hazardous Materials,** 177, 962–970.

Muzzarelh, R. A. A. (1988), Thermodynamic Study of the Interaction of NCarboxymethyl Chitosan with Divalent Metal Ions, **J. of Carbohydrate Polymers,** 221-232

Muzzarelli, R. A. A. Rocchetti, R. (1974), The use of chitosan columns for the removal of mercury from waters, **J. Chromatogr**. 96 (1974) 115-121.

Nacional, d. S. Bahía, B.Argentina, U. RMN, F. (2010), Chitosan with phosphonic and carboxylic group: New multidentate ligands, **International Journal of Polymeric Materials,** 51: 8, 711 - 720

Nicholson, John W. (1997). The chemistry of polymers. Second edition, UK: RSC PARERBACKS.

Nicole E. Z. (2009), Chelating Polymers and Environmental Remediation, **Army Research Laboratory**, 21005-5069

Nicholson, J. (2005), Polymerisation Reactions, CH: 2, **The Chemistry of Polymers,** Third Edition, John W. Nicholson, School of Science, University of Greenwich, Chatham, Kent, UK, ISBN 0–85404–684–4.

Radwan, A. A. and Alsarra, A. I. (2010), Microwave Irradiation-Assisted Synthesis of a Novel Crown Ether Crosslinked Chitosan as a Chelating Agent for Heavy Metal Ions (M+n), **Molecules***,15*, 6257-6268.

Rinaudo, M. Pavlov, G. and Desbrieres, J. (1999). Influence of acetic acid concentration on the solubilization of chitosan, **Polymer**, vol. 40, 7029-7032.

Rivas, B.; Maureira, A. (2007), Poly(2-acrylamido glycolic acid): A water-soluble polymer with ability to interact with metal ions in homogenous phase, **Inorganic Chemistry Communications**, 10, 151–154.

Rogerio, L., Thiago, G. Costa, Bruno, and S. V. Favere T. (2010), Adsorption characterization of Pb(II) and Cu(II) ions onto chitosan-tripolyphosphate beads: Kinetic, equilibrium and thermodynamic studies, **A Journal of Environmental Management**, 91, 958–969.

Rodrigues, C. A., Laranjeira, M. C. M., de-Favere, V. T., & Sadler, E.(1998). Interaction of Cu(II) on N-(2-pyridylmethyl) and N-(4-pyridylmethyl)chitosan. **Polymer**, 39(21), 5121–5126

Ruiz, M. Sastre, A.M. Guibal, E. (2000), Palladium sorption on glutaraldehyde crosslinked chitosan, **React. Funct. Polym**., 45, 155-173.

Sarhan, A. A. Ayad, D.M. Badawy, D. S. Monier, M. (2009), Phase transfer catalyzed heterogeneous N-deacetylation of chitin in alkaline solution, **React. Funct. Polym**., 69, 358-363.

Schmuckler, G. (1976). Chelate-forming resins. **Encyclopedia of polymer science and technology**. Vol. 2, 197-204. New York: Interscience.
Singh, R.B., Garg, B.S., and Singh, R.P. (1979). Oxime as spectrophotometric reagent. **Talanta**, 26, 425-4444.

Schnitzer, M. (1978), **Humic substances: Chemistry and Reactions**. Schnitzer, M. and Khan, S. U. (ed.), Soil organic matter, pp. 1-64, New York: Elsevier Scientific Publishing Company.

Skoog, D. A., Holler, F.J. (1998), principles of Instrumental Analysis. USA: Brooks/ Cole Thomson Learning.

Sugii, A., Ogawa, N., and Hashizume, H. (1979). Synthesis and properties of a new chelating resin containing the oxime group. **Talanta**, 26, 189-192.

Sposito, G. (1984), **The Surface Chemistry of Soil**, (1st Ed), Oxford: Oxford University Press.

Stevenson, F. (1982), **Humus Chemistry, Genesis, Composition, Reactions**, (1st Ed), New York: John Wiley and Sons.

Tompkin, E.R.; Sugii, A.; and Mayers, S.W. (1947). Ion exchange as a separation method. **J. Am. Chem. Soc**., 69: 2859-2865

Uhlir, L. C. Durbin, P. W. Jueng, N. and Rymond, K. N. (1993), Spacific Sequestering Agents for the Actinides. 21. Synthesis and Initial Biological Testing of Octadentate Mixed Catecholate-Hydroxypyridinonate Ligands, **J. Med. Chem**., 31, 11-18.

Vernon, F. (1977). The preparation and properties of chelating ion exchange resins. **Chemistry and Industry**, 634-637.

Vernon, F., and Nyo, K.M. (1978). Metal separations on an oxine chelating ion exchange resin**. J. Inorg. Nucl. Chem**., 40, 887-891.

Wan. W. N. Fatinathan, S. (2009), Adsorption and desorption of Cu(II), Cd(II) and Pb(II) ions using chitosan crosslinked with epichlorohydrin-triphosphate as the adsorbent, **Journal of Hazardous Materials,** 183, 233–241

Weber, W. J. and Morris, J. C. (1962), Water pollution symposium, **In: Proc. Int. Conf.**, vol. 2, Pergamon, Oxford, , 231.

Winston, A., and Mazza, E.T. (1975). Hydroxamic acic polymers. **J.Poly.Sci.Chem.Ed**, 13 (9), 2019-2030.

Wu, C. Tseng, R.-L. Juang, R.-S. (2001) Adsorption of dyes and phenols from water on the activated carbons prepared from corncob wastes, **Environ Technol**, 22: 205-213.

Xiong, C. Wu, X. and Su Z. (1996), Behavior of Macroporous Phosphonic Acid Resin Adsorbing Dysprosium (III) and its Mechanism **J. CHINESE RARE EARTHS**, 06

Yurdakoc, M. Scki, S.K. Yuedakoc (2005), Kinetic and thermodynamic studies of boron removal by Siral 5, Siral 40, and Srial 80, **J. Colloid Interf. Sci.** 286 440–446.

Zalloum, R.; Mubarak, S. (2008), Chelation properties of poly(2-hydroxy-4-acryloxybenzophenone resins toward some divalent metal ions, **Journal of Applied Polymer Science**, 109, 3180-3184.

Zhu, Y., Millan, E., and Sengupta, A.K. (1990). Toward separation of toxic metal (II) cations by chelating polymers: Some noteworthy observations. **Reactive Polymers**, 13, 241-253.

Zhoua, L. Wang, Z. Liu, Q. Huang (2009), Characteristics of equilibrium, kinetics studies for adsorption of Hg(II), Cu(II), and Ni(II) ions by thiourea-modified magnetic chitosan microspheres, **J. Hazard. Mater**, 161, 995–1002.

تحضير وتشخيص ودراسة الخواص الكلابية للكيتوسان المرتبط ب-1 هيدروكسي-2 بيريدينثايون تجاه أيونات العناصر الثقيلة.

إعداد
فريزة جميل مهنا

المشرف
الأستاذ الدكتور كمال ابراهيم أبو داري

المشرف المشارك
الأستاذ الدكتور محمد سليمان مبارك

الملخص

تمت دراسة الخواص الكلابية لمبلمر الكيتوسان- 1-هيدروكسي-2-بيريدينثيون-4-كاربوكسيلك اسيد تجاه أيونات ثنائية التكافؤ في المحاليل المائية بتغير دالة الزمن ودرجة الحموضة وكتلة الملمر وتركيز المعدن. وقد تم تحديد قدرة المبلمر على امتصاص أيونات الرصاص و النحاس والخارصين والنكيل والكادمويوم باستخدام مطيافية الامتصاص الذري
ووجد أن أعلى قدرة استعياب للمبلمر كانت عند درجة حموضة 7.0. كما تمت دراسة السلوك الحراري (عند ضغط ثابت) وحركية ادمصاص أيونات ثنائية من قبل هذا المبلمر بالنسبة لكتلة المبلمر ودرجة الحرارة ووجد أنه يمكن استعمال نموذجي لانجمير وفرندليش لوصف النتائج العلمية ولحساب الثوابت المختلفة.